

6.2.1 Fissile Material Contents

The per-package HEU mass loadings considered in the criticality evaluation range from 1000 to 36,000 g for uranium metal and from 1000 to 24,000 g for uranium oxide and UNX crystals. The HEU mass may include nonradioactive contaminants and trace elements or materials in the HEU.

The bounding types of HEU content evaluated in this criticality analysis are 4.25-in.- and 3.24-in.-diam cylinders; 2.29-in.-square bars; 1.5-in.-diam \times 2-in.-tall slugs; cubes ranging from 0.25 to 1 in. on a side; broken metal pieces of unspecified geometric shapes; skull oxide; uranium oxide; UNX crystals; and unirradiated TRIGA reactor fuel elements.

The term "broken metal pieces" is used to describe an HEU content without restrictions on shape or size other than a minimum size limit (spontaneous ignition), a maximum mass limit (criticality control), a minimum enrichment (the lower limit for HEU at 19 wt % ^{235}U in uranium), and the capacity limits of the convenience cans. The content geometry envelope encompasses regular, uniform shapes and sizes as well as irregular shapes and sizes.

The density of HEU metal ranges from 18.811 to 19.003 g/cm³ for HEU metal, corresponding to enrichments ranging from 100 to 19 wt % ^{235}U . Theoretical (crystalline) densities for HEU oxide are 10.96 g/cm³, 8.30 g/cm³, and 7.29 g/cm³ for UO_2 , U_3O_8 , and UO_3 , respectively. However, bulk densities of product oxide are typically on the order of 2.0 to 6.54 g/cm³. With increased moderation of fissile mass possible at these lower densities, only "less-than-theoretical" mass loadings would actually be achieved. Skull oxides are a mixture of U_3O_8 and graphite, having densities on the order of 2.44 g/cm³ for poured material and 2.78 g/cm³ for tamped (packed) material. Combined water saturation and crystallization of the HEU oxide is not expected in the HAC because UO_2 and UO_3 are non-hygroscopic and U_3O_8 is only mildly hygroscopic. The density of UNX crystals varies depending on the degree of hydration. The most reactive form of $\text{UO}_2(\text{NO}_3)\cdot x\text{H}_2\text{O}$ is with 6 molecules of hydration, having a density of 2.79 g/cm³. UNX crystals are highly soluble in nitric acid and mildly soluble in water. Dissolution of UNX crystals in water is assumed in this criticality evaluation. The content geometry envelope encompasses both regular, uniform clumps and densities, and irregular clumps and densities.

Table 6.1a. Summary of criticality evaluation for solid HEU metal cylinders and bars

Conditions	cylinders (d ≤ 3.24 in.) no can spacers	cylinders (d ≤ 3.24 in.) with can spacers	square bars (l,w ≤ 2.29 in.) no can spacers	cylinders (3.24 < d ≤ 4.25 in.) no can spacers	cylinders (3.24 < d ≤ 4.25 in.) with can spacers
General requirements for each fissile package (§71.55)					
“A package used for shipment of fissile material must be so designed and constructed and its contents so limited that it would be subcritical if water were to leak into the containment system, . . . so that under the following conditions, maximum reactivity of the fissile material would be attained:” (Paragraph “b”)	$k_{eff} + 2\sigma \leq 0.9228$ cvrcryt11_21_1	$k_{eff} + 2\sigma \leq 0.8866$ cvrcryt11_36_2	$k_{eff} + 2\sigma \leq 0.8787$ cvcrsq11_36_1	$k_{eff} + 2\sigma \leq 0.9215$ cvrcryct11_17_1	$k_{eff} + 2\sigma \leq 0.9202$ cvrcryct11_32_2
(1) the most reactive credible configuration consistent with the chemical and physical form of the material,	3 stacked cylinders (d = 3.24 in.) 1 cylinder per convenience can, no can spacers, 21,000g ²³⁵ U	3 stacked cylinders (d = 3.24 in.) 1 cylinder per convenience can, with can spacers, 36,000g ²³⁵ U	3 stacked bars (l,w = 2.29 in.) 1 bar per convenience can, no can spacers, 36,000g ²³⁵ U	3 stacked cylinders (d = 4.25 in.) 1 cylinder per convenience can, no can spacers, 17,000g ²³⁵ U	3 stacked cylinders (d = 4.25 in.) 1 cylinder per convenience can, with can spacers, 32,000g ²³⁵ U
(2) moderation by water to the most reactive credible extent,	flooding of the containment vessel	same	same	same	same
(3) close full reflection of the containment system by water on all sides, or such greater reflection of the containment system as may be provided by the surrounding material of the packaging.	30.48 cm H ₂ O surrounding the containment vessel	same	same	same	same

Table 6.2a. HEU fissile material mass loading limits (case name) for surface-only modes of transportation

Solid HEU metal of specified geometric shapes						
Transport index based on nuclear criticality control	cylinders (d ≤ 3.24 in.)	cylinders (3.24 in. < d ≤ 4.25 in.)	bars	slugs ^a enr. ≤ 95%	slugs ^b 80% < enr. ≤ 95%	slugs ^b enr. ≤ 80%
No can spacers						
CSI = 0.0	18,000 g ²³⁵ U (nciacyt11 18 1 3)	15,000 g ²³⁵ U (nciacyct11 15 1 3)	30,000 g ²³⁵ U (hciasqt12 30 1 3)	17,374 g ²³⁵ U (ncia5st11 1 1 7 3)	-	-
With can spacers						
CSI = 0.0	30,000 g ²³⁵ U (nciacyt11 30 2 3)	25,000 g ²³⁵ U (nciacyct11 25 2 3)	36,000 g ²³⁵ U (nciasqt11 36 2 3)	-	24,324 g ²³⁵ U (hcia70st12 2 7 3)	29,318 g ²³⁵ U (hcia5est12 2 2 5 3)
CSI = 0.4	-	-	-	-	34,749 g ²³⁵ U ^b (ncf15est11 2 2 7 3)	29,318 g ²³⁵ U (ncf15est11 2 2 5 3)
Solid HEU metal of unspecified geometric shapes characterized as broken metal ^d						
Transport index based on nuclear criticality control	95% < enr. ≤ 100%	90% < enr. ≤ 95%	80% < enr. ≤ 90%	70% < enr. ≤ 80%	60% < enr. ≤ 70%	enr. ≤ 60%
No can spacers						
CSI = 0.0	can spacers required	can spacers required	can spacers required	2,967 g ²³⁵ U (hciabmt12 4 1 5 3)	3,249 g ²³⁵ U (hciabmt12 5 1 4 3)	5,576 g Uranium (nciabmt11 6 1 3 3)
CSI = 0.4	can spacers required	can spacers required	can spacers required	5,192 g ²³⁵ U (ncf1bmt11 7 1 5 3)	5,848 g ²³⁵ U (ncf1bmt11 9 1 4 3)	14,872 g Uranium (ncf1bmt11 15 1 3 3)
CSI = 0.8	can spacers required	can spacers required	can spacers required	8,900 g ²³⁵ U (ncf2bmt11 12 1 5 3)	13,646 g ²³⁵ U (ncf2bmt11 20 1 4 3)	28,814 g Uranium (ncf2bmt11 29 1 3 3)
CSI = 2.0	can spacers required	can spacers required	can spacers required	17,059 g ²³⁵ U (ncf3bmt11 22 1 5 3)	21,444 g ²³⁵ U (ncf3bmt11 31 1 4 3)	35,320 g Uranium (ncf3bmt11 36 1 3 3)
CSI = 3.2	can spacers required	can spacers required	can spacers required	27,692 g ²³⁵ U (ncf5bmt11 35 1 5 3)	24,692 g ²³⁵ U (ncf5bmt11 36 1 4 3)	35,320 g Uranium (ncf5bmt11 36 1 3 3)
With can spacers						
CSI = 0.0	2,774 g ²³⁵ U (hciabmt12 3 2 8 3)	3,516 g ²³⁵ U (hciabmt12 4 2 7 3)	3,333 g ²³⁵ U (hciabmt12 4 2 6 3)	4,450 g ²³⁵ U (hciabmt12 6 2 5 3)	5,198 g ²³⁵ U (nciabmt11 8 2 4 3)	11,154 g Uranium (hciabmt12 12 2 3 3)
CSI = 0.4	5,549 g ²³⁵ U (ncf1bmt11 6 2 8 3)	6,154 g ²³⁵ U (ncf1bmt11 7 2 7 3)	7,500 g ²³⁵ U (ncf1bmt11 9 2 6 3)	8,900 g ²³⁵ U (ncf1bmt11 12 2 5 3)	12,996 g ²³⁵ U (ncf1bmt11 19 2 4 3)	28,813 g Uranium (ncf1bmt11 29 2 3 3)
CSI = 0.8	9,248 g ²³⁵ U (ncf2bmt11 10 2 8 3)	10,549 g ²³⁵ U (ncf2bmt11 12 2 7 3)	12,500 g ²³⁵ U (ncf2bmt11 14 2 6 3)	16,317 g ²³⁵ U (ncf2bmt11 21 2 5 3)	20,793 g ²³⁵ U (ncf2bmt11 30 2 4 3)	35,320 g Uranium (ncf2bmt11 36 2 3 3)
CSI = 2.0	13,872 g ²³⁵ U (ncf3bmt11 14 2 8 3)	18,461 g ²³⁵ U (ncf3bmt11 20 2 7 3)	20,000 g ²³⁵ U (ncf3bmt11 23 2 6 3)	25,218 g ²³⁵ U (ncf3bmt11 32 2 5 3)	24,692 g ²³⁵ U (ncf3bmt11 36 2 4 3)	35,320 g Uranium (ncf3bmt11 36 2 3 3)
CSI = 3.2	24,969 g ²³⁵ U (ncf5bmt11 25 2 8 3)	26,373 g ²³⁵ U (ncf5bmt11 28 2 7 3)	28,334 g ²³⁵ U (ncf5bmt11 35 2 6 3)	28,184 g ²³⁵ U (ncf5bmt11 36 2 5 3)	24,692 g ²³⁵ U (ncf5bmt11 36 2 4 3)	35,320 g Uranium (ncf5bmt11 36 2 3 3)

Table 6.2a. HEU fissile material mass loading limits (case name) for surface-only modes of transportation

HEU oxide and UNX crystals					
Transport index based on nuclear criticality control	HEU product oxide, no can spacers	HEU skull oxide, no can spacers	UNX crystals, no can spacers	unirradiated TRIGA fuel elements, no can spacers ^c	
				20% enrichment	70% enrichment
CSI = 0.0	21,125 g ²³⁵ U (nciaoxtl1_1_24_1_3)	15,673 g ²³⁵ U and 921 g C (nciask_9_15)	3,297 g ²³⁵ U (nciapunhct11_7_3)	921 g ²³⁵ U (nciatriga_1_15_3)	408 g ²³⁵ U (nciatriga70_1_15_3)
CSI = 0.4	-	-	11,303 g ²³⁵ U (ncflpunhct11_24_3)	-	-

- ^a When can spacers are not used, the mass limit = 17,374 g ²³⁵U.
- ^b When can spacers are used, a greater fissile mass limit is permissible based on enrichment. For CSI=0 and enrichments above 80 wt%, the fissile mass must be reduced below the volumetric limit. For CSI=0.4, fissile mass is volumetrically limited by the size of the slugs. Note that within a fixed volume, the HEU mass increases slightly with decreasing enrichment.
- ^c For ground transport, TRIGA reactor fuel element content will be limited to three fuel sections (“meats”) per loaded convenience can and up to three loaded cans per package. The TRIGA fuel content may also be configured as clad fuel rods, each rod derived from a single TRIGA fuel element. A ~15 inch long rod consists of the three fuel pellets and an exterior sheath of clad, where protruding clad at each end has been crimped in. Clad fuel rods will be packed into convenience cans, with a maximum of three fuel rods per loaded convenience can and one loaded can per containment vessel.
- ^d Uranium/aluminum and uranium/molybdenum alloys may be loaded to the broken metal mass limits by assuming the mass of the alloy is all uranium.

Table 6.2b. HEU fissile material mass loading limits for air transport mode of transportation

Solid HEU metal of specified geometric shapes					
One per convenience can	cylinders (d = 3.24 in.)	cylinders (3.24 < d ≤ 4.25 in.)	bars	slugs	
	500g ²³⁵ U	500g ²³⁵ U	500g ²³⁵ U	500g ²³⁵ U	
Solid HEU metal of unspecified geometric shapes characterized as broken metal ^a					
	enr. ≤ 20%		20% < enr. ≤ 100%		
	700g ²³⁵ U		500g ²³⁵ U		
HEU oxide, UNX crystals, unirradiated TRIGA fuel elements ^b					
	HEU product oxide	HEU skull oxide	UNX crystals	unirradiated TRIGA ^c	
				20% enrichment	70% enrichment
	not allowed	not allowed	not allowed	716g ²³⁵ U	408g ²³⁵ U

- ^a Research reactor related contents of uranium metal or U-Al alloy are packaged for air transport under these specified limits.
- ^b Research reactor related contents of U₃O₈, U₃O₈-Al, UO₂, or UO₂-Mg are packaged for air transport under limits specified for unirradiated TRIGA fuel elements. Per package limits for these items are a maximum of 716 g ²³⁵U at enrichments not exceeding 20 wt% and a maximum of 408 g ²³⁵U for content enrichments greater than 20 wt%.
- ^c For air transport, TRIGA reactor fuel element content will be limited to fuel sections or clad fuel rods as described for surface-only modes of transportation in footnote “c” of Table 6.2a and the fissile mass limit specified herein, whichever is more limiting.

the amount of hydrogenous packing material inside the containment vessel is limited to an equivalent 500 g polyethylene.

Normally, the H/X ratio inside the containment vessel is specified as an administrative control used to restrict both the amount of hydrogenous packing material normally used inside the containment vessel and other sources of moisture present in the fissile content. The total amount of hydrogen inside the containment vessel is used in the determination of package H/X ratio (i.e., the ratio of the number of hydrogen atoms "H" to the number of fissile atoms "X," where the hydrogen atoms are those of the content, including absorbed moisture and of the packing material both inside and outside of the convenience cans). However, containment vessel flooding is assumed in calculations performed for the derivation of fissile material loading limits. This simulated condition produces fissile material content that is more reactive than actual.

The 7.1–10.1 kg quantity of evaluation water required in both the NCT and HAC criticality calculations bounds reasonable amounts of hydrogenous packing material present inside the ES-3100 containment vessel for solid HEU metal content (cylinders, bars, buttons, slugs, unirradiated TRIGA fuel, and research-related fuel components fissile material). The hydrogenous packing material encompasses the solid fissile material but is not interspersed within it.

However, the 7.1–10.1 kg quantity of evaluation water does not necessarily bound reasonable amounts of hydrogenous packing material present inside the containment vessel when the fissile material is in particulate form (primarily HEU oxides and UNH crystals) or must be evaluated in particulate form (broken metal). An administrative criticality control is used to restrict the amount of hydrogenous packing material normally present inside the containment vessel (see Item 7 in Sect. 6.2.4).

6.2.4 Package Content Loading Restrictions

Loading restrictions based upon the results of the criticality safety calculations presented in Sects. 6.4 and 6.5 are as follows:

- (1) HEU fissile material to be shipped in the ES-3100 package shall be placed in stainless steel, tin-plated carbon steel or nickel-plated carbon steel convenience cans or polyethylene or Teflon bottles. The can lids may be welded, press fit, slip lid, or crimp seal types; bottle lids are screw cap type.
- (2) The content shall not exceed the "per package" fissile material mass loading limits specified in Tables 6.2a and 6.2b, and 277-4 canned spacers shall be used as indicated for criticality control. Research reactor related contents of uranium metal or U-Al alloy may be packaged for air transport under limits specified in Table 6.2b for solid HEU metal of unspecified geometric shapes characterized as broken metal. Research reactor related contents of uranium oxide and oxide compounds (U_3O_8 , U_3O_8 -Al, UO_2 , or UO_2 -Mg) may be packaged for air transport under limits specified in Table 6.2b for unirradiated TRIGA fuel elements. Per package limits for these items are a maximum of 716 g ^{235}U for content at enrichments not exceeding 20 wt% and a maximum of 408 g ^{235}U for content enrichments greater than 20 wt%.
- (3) Where 277-4 canned spacers are required, not greater than one-third of the permissible package content for that category indicated in Tables 6.2a or 6.2b shall be loaded in any vacancy between or adjacent to canned spacers inside the containment vessel. The content mass loading may be further restricted based on structural, mechanical, and practical considerations (see Sects. 1 and 2).

- (4) As shown in Fig. 1.4, the ES-3100 package may carry up to six loaded convenience cans. In situations where the plan for loading the containment vessel calls for the use of empty convenience cans to fill the containment vessel, the heavier cans shall be loaded into the bottom of the upright shipping container, and the empty cans shall be placed above them.
- (5) The presence of uranium isotopes is limited on a weight-percent basis as follows: $^{232}\text{U} \leq 40$ ppb U, $^{234}\text{U} \leq 2.0$ wt % U, $^{235}\text{U} \leq 100.0$ wt % U, and $^{236}\text{U} \leq 40.0$ wt % U.
- (6) With the exception of slug content, unirradiated TRIGA reactor fuel element content, and research reactor related content, solid HEU metal or alloy content of specified geometric shapes shall be one item per loaded convenience can. HEU bulk metal or alloy content not covered by the specified geometric shapes (cylinder, square bar, billet, slug, or unirradiated TRIGA fuel element contents) will be in the HEU broken metal category, and so limited.
- (7) The package content is defined as the HEU fissile material, bottles, the convenience cans, the can spacers, and the associated packing materials (plastic bags, pads, tape, etc.) inside the ES-3100 containment vessel. The amount of hydrogenous packing material inside the containment vessel shall not exceed an equivalent mass of 500 g polyethylene. Only non-hydrogenous packing material may be used in the containment vessel when HEU content is shipped under the broken metal category.
- (8) The mass of unidentified constituents of an HEU fissile material to be loaded into the ES-3100 will be counted against the fissile mass loading limit. The HEU fissile material will not contain unevaluated moderating materials.
- (9) The CSI is determined on the basis of the uranium enrichment and total ^{235}U mass in the package and the fissile material shape or form.

6.3 GENERAL CONSIDERATIONS

The ES-3100 packaging configuration is shown on Drawing M2E801580A031 (Appendix 1.4.8). KENO V.a modeling of this configuration with the maximum allowable contents (Sect. 6.2) for a variety of array sizes and array conditions yields bounding calculations that determine the package's CSI (Tables 6.1a–6.1e) Can spacers are used as indicated in Table 6.2a and 6.2b for the purpose of reducing neutronic interaction between the contents of the package, aiding in maintaining the $k_{\text{eff}} + 2\sigma$ below the USL for the ES-3100 package. Key input listings are provided in Appendix 6.9.7.

The HEU content of a package is in one of the following forms: metal of a specified geometric shape, metal of an unspecified shape characterized as broken metal, uranium or skull oxide, UNX crystals, or unirradiated TRIGA reactor fuel elements. The bounding types of HEU content evaluated in this criticality analysis are: 4.25-in.- and 3.24-in.-diam cylinders; 2.29-in.-square bars; 1.5-in.-diam \times 2-in.-tall slugs; cubes ranging from 0.25 to 1 in. on a side; broken metal pieces of unspecified geometric shapes; product and skull oxide; UNH crystals; and unirradiated TRIGA reactor fuel elements. Uranyl nitrate hexahydrate (UNH) has a chemical formula of $\text{UO}_2(\text{NO}_3)_2 \cdot 6\text{H}_2\text{O}$. This most reactive form is used as the bounding composition for UNX crystals in the criticality evaluation. TRIGA fuel elements are 1.44-in.-diam \times 15-in.-tall cylinders of UZrH_x containing <310 g ^{235}U . Fuel elements are sectioned into three equal length pieces. Calculations demonstrate that these contents are bounded by 3.24-in.-diam HEU metal cylinders. Evaluation of the 3.93-in.-diam \times 9.5-in.-tall U-Al cylinders is covered under the evaluation of the 4.25-in.-diam HEU metal cylinders. The evaluation of the U-Mo content is covered under the assessment of HEU contents at 95 wt % enrichment.

HEU metal shapes are distributed in an optimum arrangement in the flooded containment vessel. For the single package and the array calculations, the HEU broken metal is modeled as a homogeneous mixture of uranium metal and water filling the interior of a flooded containment vessel. This representation bounds the heterogeneous configuration of metal pieces interspersed with hydrogenous packing material inside of wrapped convenience cans. (Appendix 6.9.3., Sect. 6.9.3.1) Water soluble

several cm in thickness acts as a neutron absorber. Several inches in thickness are required for neutron multiplication to increase from neutron reflection by the stainless steel. The NCT shipping configuration model for disassembled TRIGA fuel is bounding. The same applies for TRIGA fuel with aluminum clad.

A clad fuel rod with 1.44 in. diameter fuel pellets contains 2,282.4 g UZrH_x (Appendix 6.9.3.1) and ~179 to 191 g of stainless steel. Stainless steel tends to act as a neutron absorber; moreover, its presence as clad in the TRIGA fuel content replaces water moderator otherwise present in the geometry configuration of TRIGA fuel meats. When stainless steel is homogenized with the $\text{UZrH}_{1.6}$ as in the calculation model for package content in the extremely damaged condition [10 CFR 71.55(d)(2) and 10 CFR 7155(e)(1)], the stainless steel acts more effectively as a neutron absorber. However, the amount of stainless steel added and water displaced is not expected to have a statistically significant affect on neutron multiplication. Thus, the HAC shipping configuration model for disassembled TRIGA fuel (bare fuel meats) is bounding.

A clad fuel rod with 1.41 in. diameter fuel pellets contains ~2,188 g UZrH_x and ~90 to 96 g of aluminum. While aluminum tends to act as a neutron scatter, its presence in the TRIGA fuel content replaces water moderator otherwise present in the geometry configuration of TRIGA fuel meats. The amount of aluminum added and water displaced is not sufficient to have a statistically significant affect on neutron multiplication. Thus, the HAC shipping configuration model for disassembled TRIGA fuel is also bounding for aluminum clad TRIGA fuel content.

The TRIGA content is to be transported by air; consequently, additional discussion is included in Sect. 6.7.

The 1.5-in.-diam \times 2-in.-tall slugs may be packed up to ten items per press-fit lid type convenience can and up to twelve items per crimp-lid type convenience can. With nominal dimensions, each slug weighs ~1,090 g. With $\pm 1/16$ in. tolerance on both the diameter and height, each slug in the calculation model weighs ~1218 g. As described in Appendix 6.9.1, different arrangements of slugs in the convenience cans are possible. A configuration of slugs in a flooded reflected containment vessel must be shown to be adequately subcritical and so limited either by the use of 277-4 canned spacers, by limitation of fissile mass, or by both.

Several slug arrangements depicted in Fig. 6.9.1-4b are evaluated for demonstrating that the most conservative arrangement of slugs is being analyzed. The blue marker shown in Fig. 6.9.1-4c depicts the 4.13-in. diam of the canned spacer. Content within a configuration radius of 2.125 in. (5.4 cm) are within the boundary of the convenience can wall. The convenience cans are not modeled and contents are allowed to project beyond the convenience can wall boundary. The slugs are modeled only as 100 wt % ^{235}U for this portion of the criticality evaluation. Cases **ever5st11_1_1**, **ever5est11_1_1**, **ever50st11_1**, **ever5e0st11_1**, **ever5u0st11_1**, and **ever5l0st11_1** depict very different spacing arrangements with five slugs per convenience can, three cans per package. The statistical difference in the calculated " $k_{\text{eff}} + 2\sigma$ " values is insignificant. Cases **ever6e0st11_1** and **ever6st11_1_1** depict arrangements with six slugs per convenience can, and Case **ever70st11_1** depicts seven slugs per convenience can. (Considerable deformation of the 4.25-in.-diam convenience can wall is required to achieve all but the simple pentagonal-ring arrangement of slugs.) Calculation results reveal the primary dependence of the " $k_{\text{eff}} + 2\sigma$ " value is on the fissile mass loading and the secondary dependence is on the arrangement and spacing of slugs. The calculation results presented in Table 6.9.6-8 (Appendix 6.9.6) for a flooded containment vessel indicate that only five slugs per convenience can (18,277 g ^{235}U per package) may be loaded without the use of 277-4 canned spacers (Cases **ever5st11_1_1** and **ever5est11_1_1**). Further evaluation of the single package and array configurations are required. Also, results highlighted in red indicate that 277-4 canned spacers are required for the slug content.

The sensitivity of k_{eff} to the space between slugs arranged in a pentagonal ring is evident in the calculation results for Cases **cvcr5st11_1_2** and **cvcr5est11_1_2**, which model content for three convenience cans, each location with two pentagonal rings (10 slugs) per can. These two configurations represent degrees of separation between adjacent neighbors in the pentagonal rings of 0.0 cm and 1.0 cm, respectively. The most reactive configuration occurs when the slugs are spaced 1.0 cm apart from direct contact with adjacent neighbors in the pentagonal rings. Because positioning devices are not used in the convenience cans to control spacing and prevent an optimal arrangement of contents from occurring, both calculation models for slug arrangement are the basis for additional calculations where 277-4 canned spacers may not be required.

Cases **cvcr5st11_2_1**, **cvcr5est11_2_1**, **cvcr50st11_2**, **cvcr5e0st11_2**, **cvcr5u0st11_2**, and **cvcr5l0st11_2** represent the different spacing arrangements with five slugs per convenience can, three cans per package, and cans separated by canned spacers. Likewise, Cases **cvcr6e0st11_2** and **cvcr6st11_2_1** represent arrangements with six slugs per convenience can, three can per package, and cans separated by can spacers. Case **cvcr70st11_2** represents seven slugs per convenience can. While the differences in the calculated " $k_{eff} + 2\sigma$ " values for equal numbers of slugs per can are ≤ 0.006 , the " $k_{eff} + 2\sigma$ " values are significantly below the USL. Again, the calculation results presented in Table 6.9.6-8 (Appendix 6.9.6) for these cases reveal the primary dependence of the " $k_{eff} + 2\sigma$ " value is on fissile mass loading, and the secondary dependence is on the arrangement and spacing of slugs.

Case **cvcr6e0st11_2** models three sets of slugs, six slugs in a pentagonal ring with one slug in the center, and each set of slugs separated by a 277-4 canned spacer. Cases **cv0r6e0st11_2** and **cvwr6e0st11_2** are variations of the reference case where the 1.4-in. spacer is replaced with void in the first case and is replaced with water in the second case. Comparison of the " $k_{eff} + 2\sigma$ " values between Cases **cvcr6e0st11_2** and **cv0r6e0st11_2** reveals that the spacers reduce k_{eff} by ~ 0.03 . Comparison of the " $k_{eff} + 2\sigma$ " values for Cases **cvcr6e0st11_2** and **cvwr6e0st11_2** reveals that axial spacing of the content provided by the content cans inside the containment vessel serves to reduce k_{eff} .

The calculation results presented in Table 6.9.1-8 for a flooded containment vessel indicate that up to ten slugs per convenience can (36,555 g ^{235}U per package) *might* be loaded when 277-4 canned spacers are used. Conceivable arrangements are considered in Cases **cvcr5st11_2_2**, **cvcr5est11_2_2**, **cvcr6e4st11_2**, and **cvcr73st11_2**, (Table 6.9.6-8). Suitability is contingent on the results of single package and array calculations.

Cases **ncsr5est11_2_1_1** through **ncsr5est11_2_1_15** (Appendix 6.9.6, Table 6.9.6-9) model a reflected package with one pentagonal ring of slugs per content location with 277-4 canned spacers between content locations and HEU content at 100 wt % ^{235}U . The $k_{eff} + 2\sigma$ values range from a low value of 0.688 to 0.736. These results show that the most reactive configuration is the flooded condition with MOIFR=1.0.

As shown by the cylindrical content calculation models, the ES-3100 package is not as an efficient reflector as full water reflection provided to the flooded containment vessel. This is also true for content loadings of one pentagonal ring of slugs per content location without 277-4 canned spacers between locations and HEU content at 100 wt % ^{235}U . For Cases **cvcr5est11_1_1** and **ncsr5est11_1_1_15**, the $k_{eff} + 2\sigma$ values are 0.910 and 0.871, respectively. Likewise, the $k_{eff} + 2\sigma$ values are 0.901 and 0.867 for content loadings of two pentagonal rings of slugs per content location with 277-4 canned spacers between locations, Cases **cvcr5est11_2_2** and **ncsr5est11_2_2_15**, respectively.

For the flooded containment vessel under full water reflection and loaded with the slugs in a pentagonal arrangement and 277-4 canned spacers between content locations, the $k_{eff} + 2\sigma$ value is 0.903, Case **cvcr5st11_2_2**. [10 CFR 71.55(b)] This value is below the USL value of 0.925. For packages

with the required 1.4-in. spacers, the calculated $k_{eff} + 2\sigma$ value is 0.878 for the water-reflected package, Case **ncsr5st11_2_2_15**. [10 CFR 71.55(d)] Case **hcsr5st11_02_2_15** represents the HAC model of the damaged ES-3100 package, where the outer dimensions of the package are reduced accordingly and the entire package is flooded except the neutron poison of the body weldment liner inner cavity. This single-unit case with a MOIFR = 1.0 pertains specifically to the flooded drum under conditions specified in 10 CFR 71.55(e). The $k_{eff} + 2\sigma$ value is 0.872 for this HAC. The changes in both the outer dimensions of the package and the compositions of the Kaolite and 277-4 due to HAC result in an ~ 0.001 change in the neutron multiplication factor.

6.4.2 HEU Solid Metal of Unspecified Geometric Shapes or HEU Broken Metal

Like packages with HEU metal, the neutron multiplication factor for reflected single packages with HEU broken metal increases as a function of the ^{235}U mass and the MOIFR. For example, consider the ES-3100 package loaded with three convenience cans for a total of 35,142 g ^{235}U . The $k_{eff} + 2\sigma$ values range from 0.814 to 0.891 with increasing MOIFR in the water-reflected package [Cases **ncsrbmt11_36_1_1** through **ncsrbmt11_36_1_15** (Appendix 6.9.6, Table 6.9.6-11)]. The addition of water to the package reduces the NLF, thereby increasing k_{eff} .

For the containment vessel loaded with the broken metal content but without 277-4 canned spacers between content locations, the $k_{eff} + 2\sigma$ values increase from 0.751 to 0.949 as the water content in the containment vessel increases [Cases **cvr3lha_36_1_8_1** through **cvr3lha_36_1_8_15** (Appendix 6.9.6, Table 6.9.6-10, and Appendix 6.9.3, Fig. 6.9.3.1-5)]. Cases **cvr3lha_36_1_8_15** through **cvr3lha_36_1_1_15** model the flooded containment vessel with 35 kg of broken HEU metal where the enrichment ranges from 100 to 19 wt % ^{235}U . The result for Case **cvr3lha_36_1_6_15** indicates that for an enrichment of 90 wt % ^{235}U , the mass loading cannot exceed 31,482 g in the absence of canned spacers. However, the application of this limit to higher enrichment material is non-conservative, as illustrated by the result for Case **cvr3lha_26_1_8_15**. (The results for cases highlighted in yellow indicate potential limits.) As the enrichment increases, the mass loading limit decreases (from 28,334 g to 25,894 g in this example) due to less ^{238}U for neutron absorption.

For the flooded containment vessel under full water reflection and loaded with the broken metal content and 277-4 canned spacers between content locations, the $k_{eff} + 2\sigma = 0.876$, Case **cvr3lha_36_2_8_15** [10 CFR 71.55(b)]. For packages loaded with the broken metal content and 277-4 canned spacers between content locations, the calculated $k_{eff} + 2\sigma$ value is 0.872, Case **ncsrbmt11_36_2_15** [10 CFR 71.55(d)]. Case **hcsrbmt12_36_2_15** (Appendix 6.9.6, Table 6.9.6-11) represents the HAC model of the damaged ES-3100 package, where the outer dimensions of the package are reduced accordingly and the entire package is flooded except the neutron poison of the body weldment liner inner cavity. This single-unit case with a MOIFR = 1.0 pertains specifically to the flooded drum under conditions specified in 10 CFR 71.55(e). The $k_{eff} + 2\sigma = 0.874$ for this HAC condition. The changes in both the outer dimensions of the package and the compositions of the Kaolite and 277-4 due to HAC result in an ~ 0.002 change in the neutron multiplication factor.

6.4.3 HEU Oxide

HEU product oxide content is non-hygroscopic or mildly hygroscopic. While bulk densities of product oxides are typically on the order of 6.54 g/cm³, the bulk density of HEU oxides considered for shipment in the ES-3100 ranges from 2.0 to 6.54 g/cm³. HEU skull oxide is a less dense form of U_3O_8 intermixed with graphite. Of interest are those compositions with carbon/fissile uranium (C/ ^{235}U) ratios up to 2.3×10^5 $\mu\text{g C/g}^{235}\text{U}$. The quantity of fissile uranium is extremely low where even higher C/ ^{235}U ratios are present.

HEU product oxide content may be packed in polyethylene bottles or metal convenience cans; HEU skull oxide content is packed in metal convenience cans. Polyethylene bottles and hydrogenous packing material are represented by 500 g polyethylene. While both the size and shape of the polyethylene bottles prevents the use of 277-4 canned spacers with product oxide loadings, the 10-in. height of the metal convenience cans eliminates the use of 277-4 canned spacers for product or skull oxide content packaged in these size cans. However, the convenience cans are not modeled in this criticality evaluation and this analysis is performed from the standpoint that metal-type convenience cans may be used for both oxide types.

HEU oxide content is not considered a “rigid” content like solid or broken HEU metal. For the calculation models of HEU oxides, the polyethylene is homogenized with the saturated bulk oxide. At a density of 0.9200 g/cm³, polyethylene adds 543.47826 cm³ to the volume of the saturated bulk oxide and reduces the free volume of the containment vessel by an equal amount. The evaluation water in the void region of the containment vessel fills the volume of the containment vessel that not occupied by oxide content. (The void region of the containment vessel is defined as the containment vessel volume minus the oxide content volume.) Because of the differences in densities and compositions, product oxides are addressed separately from skull oxides.

Like packages with HEU metal or broken metal, the neutron multiplication factor for reflected single packages with HEU oxide increases as a function of increasing MOIFR and decreases with decreasing ²³⁵U mass. For example, consider the ES-3100 package loaded with oxide at 6.54 g/cm³ in three convenience cans for a total of 24,000 g UO₂ (21,125 g ²³⁵U). The $k_{eff} + 2\sigma$ values range from 0.724 to 0.804 with increasing MOIFR in the reflected package [Cases **ncsrpox11_1_24_1** through **ncsrpox11_1_24_15** (Table 6.9.6-13)]. The addition of water to the package reduces the NLF, thereby increasing k_{eff} . The flooded, reflected package is the most reactive single package configuration; consequently, MOIFR is treated as a constant rather than a variable in subsequent “**pdox**” cases.

Parametric calculations are performed for oxide content loadings in a flooded, reflected package by varying the oxide bulk density from 6.54 g/cm³ to a lower value limited by the capacity of the convenience cans. The maximum content capacity of the ES-3100 is ~6,975 cm³, where each of three 4.25-in.-diam × 10.0-in.-tall convenience cans has a capacity of ~2,375 cm³. As shown in Table 6.9.6-13a, calculations for a loading of 24,000 g UO₂ are performed at bulk densities of 6.54 g/cm³, 5.0 g/cm³, and 4.0 g/cm³, but not 3.0 g/cm³ because the capacity of the convenience cans is exceeded for this mass loading. Note that Case **ncsrpox11_1_24_15** (Table 6.9.6-13) is identical to Case **ncsrpdox11_1_5_24** (Table 6.9.6-13a). Results for the parametric Cases **ncsrpdox11_1_n_24**, **ncsrpdox11_1_n_20**, and **ncsrpdox11_1_n_15** reveal the consistent increase in the $k_{eff} + 2\sigma$ values as the bulk density decreases. This increase in neutron multiplication is due to the increased moderation of the HEU oxide.

Cases **ncsrpdox11_1_n_14** for UO₂ (12,323 g ²³⁵U), **ncsrpdox11_2_n_14** for U₃O₈ (11,850 g ²³⁵U), and **ncsrpdox11_3_n_14** for UO₃ (11,627 g ²³⁵U) evaluate the ES-3100 package loaded with 14 kg oxide over the range of bulk density “*n*”. The $k_{eff} + 2\sigma$ values reveal a consistent increase over the range of density. Results for Cases **ncsrpdox11_2_1_14** and **ncsrpdox11_3_1_14** indicate that both the U₃O₈ content ($k_{eff} + 2\sigma = 0.778$) and the UO₃ content ($k_{eff} + 2\sigma = 0.760$) are bounded by the UO₂ content ($k_{eff} + 2\sigma = 0.814$). Even though the capacity of the convenience cans is exceeded by 25 g, these cases are retained for the purpose of illustrating this point.

Results for a reflected containment vessel loaded with HEU oxide reveal the same trends in the $k_{eff} + 2\sigma$ values as do results for the reflected package; however, the $k_{eff} + 2\sigma$ values are ~0.1 greater in the containment vessel cases. For the flooded containment vessel loaded with UO₂, the $k_{eff} + 2\sigma$ values increase from 0.838 to 0.911 with decreasing bulk density [Cases **everpdox11_1_5_14_15** through

cverpdoxt11_1_1_14_15 (Table 6.9.6-12 and Fig. 6.9.1-6)]. For the dry containment vessel, the $k_{eff} + 2\sigma$ values increase from 0.824 to 0.912 [Cases **cverpdoxt11_1_5_14_1** through **cverpdoxt11_1_1_14_1** (Table 6.9.6-12 and Fig. 6.9.1-6)]. Comparison of results for high density UO_2 oxide saturated with 862 g water reveals a small increase in $k_{eff} + 2\sigma$ from 0.824 to 0.838 due to flooding of the containment vessel. Comparison of results for low density UO_2 oxide saturated with 5,712 g water reveals an insignificant increase in $k_{eff} + 2\sigma$ due to flooding of the containment vessel, [Cases **cverpdoxt11_1_5_14_15** and **cverpdoxt11_1_5_14_1** (Table 6.9.6-12 and Fig. 6.9.1-6)].

Cases **cverpdoxt11_1_11_14_15** through **cverpdoxt11_1_1_14_15** demonstrate that the $k_{eff} + 2\sigma$ values decrease for decreased mass loadings of HEU oxide at constant bulk density.

For the flooded containment vessel under full water reflection containment, the $k_{eff} + 2\sigma$ value is 0.914, Case **cverpdoxt11_1_3_24_15**. [10 CFR 71.55(b)] The $k_{eff} + 2\sigma$ value is 0.817 for water-reflected package, Case **ncsrpdoxt11_1_3_24**. [10 CFR 71.55(d)] Case **hcsrpdoxt12_1_3_24** (Table 6.9.6-13a) represents the HAC model of the damaged ES-3100 package, where the outer dimensions of the package are reduced accordingly and the entire package is flooded except the neutron poison of the body weldment liner inner cavity. This single-unit case pertains specifically to the flooded drum under conditions specified in 10 CFR 71.55(e). The $k_{eff} + 2\sigma$ value is 0.819 for this HAC condition. The changes in both the outer dimensions of the package and the compositions of the Kaolite and 277-4 due to HAC result in an ~ 0.002 change in the neutron multiplication factor.

Cases **cversk3cc_1_15_17** through **cversk3cc_10_15_17** (Appendix 6.9.6, Table 6.9.6-17) evaluate the 10 skull oxide compositions identified Table 6.9.3.1-3b, where the containment vessel is loaded with 3 convenience cans. The fissile enrichment is ~ 70 wt % ^{235}U for contents “**sk3cc_1**” through “**sk3cc_5**” and ~ 38 wt % ^{235}U for contents “**sk3cc_6**” through “**sk3cc_8**.” The observed maximums of 7.1 kg skull oxide and ~ 93.2 wt % ^{235}U enrichment present in 292 convenience cans are the basis for the hypothetical contents “**sk3cc_9**” and “**sk3cc_10**,” where unidentified material is treated as ^{235}U and the carbon content is either maximized or minimized. Content “**sk3cc_10**” differs from “**sk3cc_9**” in that 921 g of graphite in the skull oxide is replaced with 921 g ^{235}U in the form of U_3O_8 . Content “**sk3cc_10**” is more representative of high enrichment skull oxides where < 85 g of graphite is present. For each of the 10 content models, 513 g of the skull oxide content is modeled as polyethylene, representing the potential use of hydrogenous packing material. The U_3O_8 content ranges from 8 to 21 kg, while the ^{235}U content ranges from 3.7 to 16.4 kg. The graphite content ranges from 0 to 921 g C, and the C/ ^{235}U ratio ranges from 0 to 223,432 μg C/g ^{235}U . For Cases **cversk3cc_1_15_17** through **cversk3cc_10_15_17** at both saturation moisture and full graphite content, the $k_{eff} + 2\sigma$ values range from 0.759 to 0.855 in the flooded, water-reflected containment vessel. Cases **cversk3cc_9_15_17** and **cversk3cc_10_15_17** reveal that $k_{eff} + 2\sigma$ increases slightly when the 921 g of carbon in the skull oxide is replaced with 726 g ^{235}U in the form of U_3O_8 .

Cases **cversk3cc_4_1_1** through **cversk3cc_4_m_g** evaluate the effects of moisture and skull oxide graphite content on reactivity. The case designator “**m**” ranges from 1 to 15, signifying the variation in moisture; “**g**” ranges from 1 to 17, signifying the variation in graphite. Examination of results indicates that moisture content has a predominate effect on the neutron multiplication factor, while variation in graphite content has a minor effect. The peak $k_{eff} + 2\sigma$ value occurs at saturated moisture and full graphite content.

Cases **ncsrsk_1_15** through **ncsrsk_10_15** (Appendix 6.9.6, Table 6.9.6-18a) model the 10 skull oxide compositions in a flooded containment vessel in a water reflected package. The $k_{eff} + 2\sigma$ values range from 0.641 to 0.745. Likewise, Cases **hcsrsk_1_15** through **hcsrsk_10_15** (Appendix 6.9.6, Table 6.9.6-18b) evaluate infinite arrays damage packages. The $k_{eff} + 2\sigma$ values ranging from 0.658 to 0.767 are not statistically significantly different from the NCT case results.

Cases **ncsrsk_9_1** through **ncsrsk_9_15** evaluate the bounding skull oxide content containing ~19.9 kg U_3O_8 and 921 g graphite, where the saturation moisture is varied from 0 to 3801 g water. Likewise, Cases **ncsrsk_10_1** through **ncsrsk_10_15** evaluate the skull oxide content containing ~20.8 kg U_3O_8 where the 921 g of graphite in the skull oxide is replaced with 726 g ^{235}U in the form of U_3O_8 . The $k_{eff} + 2\sigma$ values range from 0.403 to 0.741 in the former set of cases and range from 0.404 to 0.746 in the latter set of cases. The $k_{eff} + 2\sigma$ values are well below the USL value of 0.925, indicating that canned spacers are not required for criticality control. Moreover, these results indicate that moisture content has a predominate effect on the neutron multiplication factor, while the graphite content has an insignificant effect.

6.4.4 UNH Crystals

UNH crystal content is to be packed in Teflon bottles, which may be placed in polyethylene bags. The Teflon bottles are not credited for containing the UNH crystal content. The 277-4 canned spacers are not used in this packing configuration. Teflon is polytetrafluoroethylene (or Polyethylene Tetrafluoride) having a monomer formula of C_2F_4 with a melting point of ~280°C (536°F). Teflon will not melt at the much lower containment vessel inner wall temperatures associated with NCT and HAC. The use of Teflon and polyethylene packing material is conservatively represented by 500 g of polyethylene in the calculation model. UNH crystal content is not considered a "rigid" content like solid or broken HEU metal. Like HEU oxide content, the UNH crystal content is homogenized with the polyethylene.

Unlike the other HEU contents, UNH crystals are soluble in water. The most reactive content condition occurs at an optimum solution concentration derived from the UNH crystal loading and the volume of water flooding the containment vessel. Both flooding of the containment vessel and a reduced loading of UNH crystals going into solution is required to achieve the most reactive configuration.

Consider a flooded containment vessel with the UNH crystals in solution and no polyethylene. For Cases **everunhct11_24_1** through **everunhct11_1_1** (Table 6.9.6-14), the $k_{eff} + 2\sigma$ values range from 0.823 to 0.609 and optimum concentration occurs at ~9,000 g UNH (Case **everunhct11_9_1**, $k_{eff} + 2\sigma = 0.857$). Consider a flooded containment vessel with a solution of UNH crystals homogenized with 500 g polyethylene. For Cases **everpunhct11_24_15** through **everpunhct11_1_15** (Table 6.9.6-14), the $k_{eff} + 2\sigma$ values range from 0.827 to 0.613 and optimum concentration occurs at ~10,000 g UNH (Case **everpunhct11_10_15**, $k_{eff} + 2\sigma = 0.863$). The replacement of water with 500 g of polyethylene in the latter set of cases results in changes to the neutron multiplication factor on the order of ~0.004 to 0.006. The concentration for a 24,000 g loading in both set of cases is 1,106 g ^{235}U per liter of flooded containment vessel. In the calculation of the uranium concentration, the solution volume is not reduced by the volume of polyethylene because polyethylene is homogenized with UNH in the solution.

For Cases **everpunhct11_24_1** through **everpunhct11_1_1** (Table 6.9.6-14), the homogenized UNH crystals and polyethylene are dispersed over a dry containment vessel. The $k_{eff} + 2\sigma$ values range from 0.769 to 0.251 as the mass loading decreases. Comparison with results for corresponding Cases **everpunhct11_24_15** through **everpunhct11_1_15** for a flooded containment vessel reveals that the most reactive content condition occurs for UNH in the solution state.

For Cases **everbpunhct11_24_15** through **everbpunhct11_1_15** (Table 6.9.6-14), homogenized UNH crystals and polyethylene are settled on the bottom of the containment vessel and the residual volume above it is flooded. The $k_{eff} + 2\sigma$ values range from 0.817 to 0.553 as the mass loading decreases. For Cases **everbpunhct11_24_1** through **everbpunhct11_1_1**, the residual volume above the content is dry. Likewise, the $k_{eff} + 2\sigma$ values range from 0.815 to 0.478 as the mass loading decreases.

Comparison of results for corresponding Cases **cvdrpunhct11_n_1** and **cvrbpunhct11_n_15** reveal greater changes in the k_{eff} values occurring at the lower mass loadings when dispersed content is settled to the bottom of the containment vessel. Nevertheless, interspersed moderation has a dominant effect on k_{eff} occurring when settled content goes into solution (Case **cvrbpunhct11_10_15** vs Case **cvcrpunhct11_10_15**).

Similar to packages loaded with HEU metal, broken metal, or oxide, the neutron multiplication factor for a reflected single package with UNH crystals increases as a function of MOIFR. Consider the ES-3100 package loaded with bottles for a total of 24,000 g UNH crystals (11,303 g ^{235}U). For Cases **ncsrnunct11_24_1_1** through **ncsrnunct11_24_1_15** (Table 6.9.6-15), the $k_{eff} + 2\sigma$ values range from 0.605 to 0.702 with increasing MOIFR in the water-reflected package. For Cases **ncsrpunhct11_24_1** and **ncsrpunhct11_24_15** (Table 6.9.6-15), the $k_{eff} + 2\sigma$ values range from 0.609 to 0.708 with increasing MOIFR in the water-reflected package. These cases confirm that the replacement of water with 500 g of polyethylene results in changes to the neutron multiplication factor on the order of ~ 0.004 to 0.006.

For a flooded containment vessel with UNH crystals in solution, the $k_{eff} + 2\sigma$ values range from 0.702 to 0.646 [Cases **ncsrnunct11_24_1_15** through **ncsrnunct11_2_1_15** (Table 6.9.6-15)]. Similarly, for a flooded containment vessel with a solution of UNH crystals homogenized with 500 g of polyethylene, the $k_{eff} + 2\sigma$ values range from 0.708 to 0.545 [Cases **ncsrpunhct11_24_15** through **ncsrpunhct11_1_15** (Table 6.9.6-15)]. At optimal concentration ($\sim 8,000$ g UNH), the calculated $k_{eff} + 2\sigma$ value is 0.863 for Case **cvcrpunhct11_10_15** and $k_{eff} + 2\sigma = 0.753$ for Case **ncsrpunhct11_8_15**. The water-reflected containment vessel is more reactive than the water-reflected package; therefore, the result for Case **cvcrpunhct11_10_15** is reported. [10 CFR 71.55(b)] The result for Case **ncsrpunhct11_8_15** having the maximum $k_{eff} + 2\sigma$ value is reported for the NCT water-reflected package. [10 CFR 71.55(d)]

Unlike solid HEU metal and oxide content, which are confined to the containment vessel and only water leakage into the containment vessel need be considered, the evaluation of UNH crystal content for compliance with 10 CFR 71.55(b) also requires that the leakage of liquid HEU contents out of the containment be addressed. This is because UNH crystals are soluble in water and would dissolve in the water flooding the containment vessel and the containment vessel well. For a content loading of 24,000 g UNH, the uranium concentration inside the containment vessel drops from 1,106 g $^{235}\text{U/L}$ to 710 g $^{235}\text{U/L}$. Optimum solution concentrations occurs for fissile mass loadings of $\sim 15,000$ g UNH. In the calculation of the uranium concentration, the solution volume is not reduced by the volume of polyethylene because polyethylene is homogenized with UNH in the solution.

Cases **hesrpunhct12_8_15** (Table 6.9.6-15) and **icsrpunhct12_15_15** (Table 6.9.6-16) represent the HAC model of the damaged ES-3100 package where the outer dimensions of the package are reduced accordingly. For Case **hesrpunhct12_8_15**, the dilution of the UNH crystals is confined to the containment vessel, and maximum reactivity occurs at ~ 8000 g UNH homogenized with 500 g polyethylene. For Case **icsrpunhct12_15_15**, UNH crystals are dissolved in the water flooding the containment vessel and the containment vessel well. The fissile material is uniformly distributed over the volume of the containment vessel and the well, but the polyethylene is confined to the containment vessel. Maximum reactivity occurs at $\sim 15,000$ g UNH. These single-unit cases with a MOIFR = 1.0 pertain specifically to the flooded drum under conditions specified in 10 CFR 71.55(e), where the $k_{eff} + 2\sigma$ values are 0.752 and 0.814 for this HAC condition. The result for Case **icsrpunhct12_15_15** having the maximum $k_{eff} + 2\sigma$ value is reported for the HAC water-reflected package. [10 CFR 71.55(e)]

6.5 EVALUATION OF PACKAGE ARRAYS UNDER NORMAL CONDITIONS OF TRANSPORT

For the NCT array evaluation of ES-3100 packages, the package content is confined within the containment vessel, consistent with the result of the tests specified in §71.71 (Normal Conditions of Transport). The array sizes examined in this evaluation are infinite, $13 \times 13 \times 6$, $9 \times 9 \times 4$, $7 \times 7 \times 3$, $5 \times 5 \times 2$, **ETP 27×3** , and the degenerate single unit. The “N” and corresponding CSI values for arrays determined to be adequately subcritical are as follows: $N = \infty$, CSI = 0; $N = 202$, CSI = **0.3**; $N = 64$, CSI = 0.8; $N = 29$, CSI = 1.7; ~~$N = 10$, CSI = 5.0~~; and $N = 16$, CSI = 3.2. All arrays, except the infinite array, are reflected with 30 cm (1 ft) of water. These arrays are nearly cubic in shape for optimum array reactivity, thus eliminating the need for placing criticality controls on package arrangements in terms of stack height, width, and depth of an array. The array configurations and the range of water contents (Table 6.4) evaluated bound all possible packaging arrangements and moderation conditions for NCT.

6.5.1 Solid HEU Metal of Specified Geometric Shapes

For infinite and finite arrays of packages with HEU metal, the neutron multiplication factor increases as a function of the ^{235}U mass and decreases as a function of MOIFR. For example, consider the ES-3100 package loaded with three convenience cans for a total of 36,000 g ^{235}U where each can contains a 3.24-in.-diam cylinder. For package content without 277-4 canned spacers, the $k_{\text{eff}} + 2\sigma$ values range from 1.027 to 0.963 with increasing MOIFR in the package [Cases **nciacyt11_36_1_1** through **nciacyt11_36_1_15** (Appendix 6.9.6, Table 6.9.6-3)]. For package content with 277-4 canned spacers, the $k_{\text{eff}} + 2\sigma$ values range from 0.957 to 0.880 with increasing MOIFR in the package [Cases **nciacyt11_36_2_1** through **nciacyt11_36_2_15** (Appendix 6.9.6, Table 6.9.6-3)].

The effect of increasing the water content of the array is straightforward. As interspersed water is added to the packages of an array, two reactivity effects occur in series. The first effect is the tendency for reactivity to remain constant due to controlled neutron interaction between the packages of the array. For an infinite array where neutrons cannot escape from the system, neutrons are scattered about the array. In the MOIFR range of $1\text{e-}20$ to $1\text{e-}02$, both the interspersed moderator inside the packages of the dry array and the interstitial moderator between the package drums of the array are not sufficient for neutron thermalization and absorption to occur in the adjacent packaging materials. However, hydrogen in the 277-4 provides moderation, and neutrons are absorbed in the interspersed boron of this neutron poison. This results in a subcritical system with near constant neutron multiplication factors over the range of MOIFR. The second effect is the tendency for reactivity to decrease due to internal moderation in packages of the array. The introduction of water above ~ 0.01 MOIFR shows the effect of isolating the individual array units from each other. The neutron multiplication factor approaches k_{eff} for the single, water-reflected unit at a full-content water fraction (MOIFR = 1.0).

The array case with a water fraction of MOIFR = $1\text{e-}04$ pertains specifically to packages under NCT where the Kaolite and recesses of the package external to the containment vessel do not contain any residual moisture. This NCT case is more reactive than all other NCT cases where more moisture is present in the Kaolite and recesses of the package. Interspersed water between the containment vessels in the array will reduce neutronic interaction between the flooded contents because neutrons are absorbed in the hydrogen of the water. As more water is added, the packages of the array become isolated, and array reactivity ($k_{\text{eff}} + 2\sigma = 0.880$, Case **nciacyt11_36_2_15**) approaches the reactivity of the single unit ($k_{\text{eff}} + 2\sigma = 0.873$, Case **ncsrcyt11_36_2_15**).

Repeated for 4.25-in.-diam cylinders (Appendix 6.9.6, Table 6.9.6-7); 2.29-in. -square bars (Table 6.9.6-5); and 1.5-in.-diam \times 2-in.-tall slugs (Table 6.9.6-9), this type of analysis for the 3.24-in.-diam cylinders demonstrates that arrays of packages with restricted fissile material (^{235}U)

loading remain subcritical over the entire range of water content or MOIFR. HEU bulk metal or alloy content not covered by the specified geometric shapes (cylinder, square bar, or slug contents) will be in the HEU broken metal category, and so limited.

Cases **nciatriga_1_1_3** through **nciatriga_1_15_3** (Appendix 6.9.6, Table 6.9.6-20a) represent infinite arrays of packages containing the bounding TRIGA fuel content (20 % enrichment with 45 wt % U containing 307 g ²³⁵U), without 277-4 canned spacers. The MOIFR is set at 1.0e-04 such that neutronic interaction between packages is maximized. For these cases, the $k_{eff} + 2\sigma$ values increase from 0.218 to 0.525 as MOIFR increases. The $k_{eff} + 2\sigma = 0.525$ for Case **nciatriga_1_15_3** is substantially below the USL value of 0.925, indicating that canned spacers are not required for criticality control.

As stated in Sect. 6.4.1, 10 CFR 71.55(d)(2) requires the geometric form of a package's content not be substantially altered under the NCT. Similarly, 10 CFR 71.55(e)(1) requires that the package be adequately subcritical under HAC with the package contents in the most reactive credible configuration. Even though visible signs of damage to the metal convenience can have not been observed resulting from the regulatory tests, conclusions about damage to the TRIGA fuel content are not extrapolated from test data. The regulatory requirements are addressed by modeling the TRIGA fuel content in an extremely damaged condition. A series of criticality calculations is performed for making a determination of subcriticality. Cases **nciat55d2_1_1_3** through **nciat55d2_1_15_3** (Appendix 6.9.6, Table 6.9.6-20d) represent TRIGA fuel content homogenized with variable density water over the free volume of the containment vessel. The packaging is flooded in each ES-3100 package of the infinite array. The variable density water ranges from the dry containment condition to the fully flooded condition. Credit for physical integrity of the content is not taken in this set of cases which model the substantially altered content. The calculation results in Table 6.9.6-20d indicate extremely damaged content (Case **nciat55d2_1_15_3** with $k_{eff} + 2\sigma = 0.716$) is more reactive than the unaltered configuration (Case **nciatriga_1_15_3** with $k_{eff} + 2\sigma = 0.442$). Nevertheless, both cases are adequately below the USL of 0.925 and the requirement of 10 CFR 71.55(d)(2) is satisfied. Given that changes external to the containment vessel due to the HAC do not result in an appreciable change in neutron multiplication for an array of packages, similar results are expected for the cases demonstrating compliance with 10 CFR 71.55(e)(1).

For TRIGA fuel content as clad fuel rods, the amount of clad added (stainless steel as a neutron absorber or aluminum as a neutron scatter) and corresponding amount of water moderator displaced by the clad is not expected to have a statistically significant affect on the calculated k_{eff} . Thus, the NCT shipping configuration model for disassembled TRIGA fuel (bare fuel meats) bounds shipping configuration model for TRIGA fuel configured as clad fuel rods (Appendix 6.9.3.1).

The array results for three slug configurations presented in Table 6.9.6-9 (Appendix 6.9.6) are for five or ten slugs touching or spaced apart in a pentagonal ring (Cases **ncia5st11** and **ncia5est11**) and for seven slugs formed by a hexagonal ring of slugs with one slug in the center of the ring (**ncia70st11**). These cases are used to establish the mass loading limitations, which in turn limit the number of slugs in the package to less than the number required to assemble a critical configuration.

Cases **ncia5est11_1_1_8_3** through **ncia5est11_1_1_1_3** (Appendix 6.9.6, Table 6.9.6-9) represent infinite arrays of packages containing 18,277 g U without 277-4 canned spacers. For these cases, the $k_{eff} + 2\sigma$ values increase from 0.550 to 0.924 as the enrichment is increased from 19.0 wt % to 100.0 wt % ²³⁵U. The $k_{eff} + 2\sigma$ value is 0.924 for Case **ncia5est11_1_1_8_3**, which is below the USL of 0.925. Likewise, the $k_{eff} + 2\sigma$ values for Cases **ncia5st11_1_1_8_3** through **ncia5st11_1_1_1_3** increase from 0.521 to 0.929 as the enrichment is increased. However, the $k_{eff} + 2\sigma$ value is 0.929 for Case **ncia5st11_1_1_8_3**, which is slightly above the USL of 0.925. For simplification of the criticality

evaluation, the maximum enrichment is limited to 95% and the corresponding fissile mass limit is 17,374 g ^{235}U . For Cases **ncia5st11_1_1_7_3** and **ncia5est11_1_1_7_3**, the $k_{\text{eff}} + 2\sigma$ values are below the USL. Moreover, the values are not statistically different.

Cases **ncia70st11_2_8_3** through **ncia70st11_2_1_3** (Appendix 6.9.6, Table 6.9.6-9) represent infinite arrays of packages containing 25,588 g U with 277-4 canned spacers. For these cases, the $k_{\text{eff}} + 2\sigma$ values increase from 0.473 to 0.915 as the enrichment is increased from 19.0 wt % to 100.0 wt % ^{235}U . The $k_{\text{eff}} + 2\sigma$ value of 0.894 for Case **ncia70st11_2_7_3** at the 95% enrichment limit is adequately below the USL of 0.925.

Cases **ncia5est11_2_2_8_3** through **ncia5est11_2_2_1_3** (Appendix 6.9.6, Table 6.9.6-9) represent infinite arrays of packages containing 36,555 g ^{235}U with 277-4 canned spacers. For these cases, the $k_{\text{eff}} + 2\sigma$ values increase from 0.583 to 0.983 as the enrichment is increased from 19.0 wt % to 100.0 wt % ^{235}U . At 80 wt % ^{235}U , the $k_{\text{eff}} + 2\sigma$ value (0.908) for Case **ncia5est11_2_2_5_3** with spaced-apart slugs is just below the USL. Similarly, Case **ncia5st11_2_2_5_3** with touching slugs has a calculated $k_{\text{eff}} + 2\sigma$ value of 0.902. Therefore, a restriction on mass and enrichment for slug content is that for ≤ 80 wt % ^{235}U , the mass of ^{235}U in the package must not exceed 29,318 g as a prerequisite for the shipment of the package slug content and with 277-4 canned spacers under a CSI = 0.0.

Cases **ncf15est11_2_2_8_3** through **ncf15est11_2_2_1_3** (Appendix 6.9.6, Table 6.9.6-9) represent a $13 \times 13 \times 6$ array of packages containing 36,555 g ^{235}U with 277-4 canned spacers for which the corresponding rounded CSI = 0.4. For these cases, the $k_{\text{eff}} + 2\sigma$ values increase from 0.548 to 0.938 as the enrichment is increased from 19.0 wt % to 100.0 wt % ^{235}U . Case **ncf15est11_2_2_7_3** at 95 wt % ^{235}U with $k_{\text{eff}} + 2\sigma = 0.920$ is below the USL of 0.925 to permit increasing the limit on enrichment for mass loadings of ≤ 34.7 kg uranium metal.

The CSI determinations provided in this section are contingent upon satisfactory results under the HAC evaluation (Sect. 6.6.1).

6.5.2 HEU Solid Metal of Unspecified Geometric Shapes or HEU Broken Metal

Like packages with HEU metal, the neutron multiplication factor for arrays of packages with HEU broken metal decreases as a function of MOIFR and increases as a function of the ^{235}U mass. For example, consider the ES-3100 package loaded with three convenience cans for a total of 35,142 g ^{235}U and no canned spacers between content locations. The $k_{\text{eff}} + 2\sigma$ values range from 1.138 to 0.913 with increasing MOIFR [Cases **nciabmt11_36_1_8_1** through **nciabmt11_36_1_8_15** (Appendix 6.9.6, Table 6.9.6-11)]. The introduction of water above ~ 0.01 MOIFR shows the effect of isolating the individual array units from each other. Array reactivity ($k_{\text{eff}} + 2\sigma = 0.913$) approaches the reactivity of the water-saturated, water-reflected single package Case **ncsrbmt11_36_1_15** ($k_{\text{eff}} + 2\sigma = 0.891$).

In the series of calculations using the ES-3100 package model with NCT geometry (Cases **nciabmt11_1_n_m_3** through **nciabmt11_36_n_m_3**), the enrichment of the content is varied from 19 wt % to 100 wt % ^{235}U . These array cases with a water fraction of MOIFR = $1\text{e-}04$ pertain specifically to NCT packages where both the neutron poison of the body weldment liner inner cavity and the Kaolite are dry (in the as-manufactured condition) and both the recesses of the package external to the containment vessel and the interstitial space between the drums of the array do not contain any residual moisture. As stated before, this NCT case is more reactive than all other NCT cases where more moisture is present in the Kaolite and recesses of the package. Increased interspersed water between the containment vessels in the array will reduce neutronic interaction between the flooded contents to a point where the packages of the array become isolated.

Ranges of enrichment are specified in Table 6.1b (10 CFR 71.59) for identifying fissile mass loading limits for HEU broken metal. Consider specifically enrichments >95 wt % ^{235}U . The containment vessel calculations (Case **cvr3lha_36_1_8_15** versus Case **cvr3lha_36_2_8_15**) indicate that 277-4 canned spacers are required in this enrichment range, where the maximum evaluated fissile mass loading of 35,142 g ^{235}U is possible. However, the fissile mass loading must be limited to 2,774 g ^{235}U (Case **nciabmt11_3_2_8_3**) in order for the $k_{eff} + 2\sigma$ value ($= 0.904$) to be below the USL of 0.925. This fissile mass limit is conservative when applied to enrichments only slightly greater than 95 wt % ^{235}U . A reduction in the enrichment within the range of 80 to 95 wt % ^{235}U (Cases **nciabmt11_4_2_7_3** and **nciabmt11_4_2_6_3**) does not result in a sufficient reduction in the $k_{eff} + 2\sigma$ from neutron absorption in ^{238}U to allow for increased mass loadings. Therefore, the uranium mass limit remains at ~ 2774 g, while the fissile mass loading limit decreases with the reduction in enrichment as illustrated in Table 6.1b. As stated previously, these fissile mass loading limits for a $\text{CSI} = 0$ are contingent upon the infinite array of damaged packages also being adequately subcritical for HAC (Sect. 6.6.2).

This evaluation technique for determination of mass loading limits for enrichment intervals is repeated over the range of HEU enrichments identified in Table 6.1b. At HEU enrichment <60 wt % ^{235}U , the evaluated package mass loading limit of 35 kg uranium is achieved, so further delineation of fissile mass loading limits is not required.

The loading limits for HEU solid metal of unspecified geometric shapes or for HEU broken metal are summarized in Table 6.2a based on array calculations performed using the uniform dispersal approximation "cha" model (Fig. 6.9.1-5d). The calculation results on which the determination of the loading limits is based are summarized in Table 6.1c.

As discussed in Appendix 6.9.1, the "cha" model is a first-order approximation model. The 500 g polyethylene representing the use of hydrogenous packing material is replaced with water in the flooded containment vessel. Broken metal and water is homogenized as a uranium "solution" and uniformly dispersed over the entire volume of the containment vessel. The vertical location of the 277-4 canned spacers inside the containment vessel is based on a fixed HEU packing fraction of ~ 0.59 . The use of this large packing fraction results in minimum separation between canned spacers, which minimizes the size of the lower and middle content locations and maximizes the size of the upper content location. Reactivity of the containment vessel is driven by the oversized upper content location having a proportionately greater amount of fissile material. Conversely, the use of a small packing fraction (~ 0.2) in the "cha" model would result in greater separation between the canned spacers, which increases the size of the lower and middle content locations while reducing the size of the upper content location. Reactivity of the containment vessel would decrease as the proportions of fissile material in the content regions equalize. Calculations based on a packing fraction of ~ 0.59 bound similar cases based on lower packing fractions.

The "cha" model is characteristic of the situation where the dimensions of the broken metal pieces are sufficiently small to allow pieces of HEU to pass between the void spaces formed between the inner wall of the containment vessel and the exterior wall of the canned spacers.

As shown in Fig. 6.9.3.1-3, HEU broken metal content typically consists of irregular pieces, sufficiently large (0.5 in. to several inches on a side), that will not pass between the 277-4 canned spacer locations. The packing fraction calculation model "fl" and the dispersed content calculation model "fd" better represent broken metal content which does not pass between the canned spacer locations. Inside the containment vessel, the content locations between canned spacers are established based on a variable packing fraction for HEU broken metal ranging from 0.2 to 0.6. The 500 g polyethylene is included in the flooded containment vessel. HEU broken metal, polyethylene and water are homogenized as a

uranium “solution” residing within the content locations (Figs. 6.9.1-5e and 6.9.1-5f) rather than distributed uniformly over the containment vessel (Fig. 6.9.1-5d). The “**fl**” model defines the upper content location based on packing fraction while the “**fd**” model defines the upper content location as the entire region above the upper canned spacer.

NCT cases for the “**fl**” and “**fd**” calculation models are documented in Table 6.9.6-11b. The reference case results based on the uniform dispersal approximation “**cha**” model are highlighted. The corresponding cases for the packaging fraction (“**fl**”) and for the dispersed content (“**fd**”) calculation models are given in the rows below the reference case. Consider Case **nciabmt11_4_1_5_3** where the quantity of HEU content in the model is calculated based on a discrete number of 1-in. cubes. The HEU in corresponding Cases **nciapbmtfl11_1_n_4_5** and **nciapbmtfd11_1_n_4_5** is not limited to fractional kilogram quantities based on whole cubes as in Case **nciabmt11_4_1_5_3**. Instead, the intended whole kilogram quantities of HEU are evaluated as a function of the packing fraction (“**n**”) in the “... flt11_1_n_...” and “... fdt11_1_n_...” cases.

An increase of ~ 0.08 in the $k_{eff} + 2\sigma$ values is observed as the packing fraction is reduced and more water is homogenized with the fissile material, (i.e., Cases **nciapbmtfl11_1_6_4_5** through **nciapbmtfl11_1_2_4_5**, Table 6.9.6-11b). As the packing fraction is reduced and the volume of the content location increases accordingly, neutron multiplication increases due to increased moderation of the fissile material. A considerable increase of ~ 0.22 in the $k_{eff} + 2\sigma$ values is observed when fissile material in the upper can location is homogenized with water in the upper content location and dispersed over that region, (i.e., Case **nciapbmtfl11_1_6_4_5** vs Case **nciapbmtfd11_1_6_4_5**, Table 6.9.6-11b). Nevertheless, the $k_{eff} + 2\sigma$ values for the packaging fraction “**fl**” and dispersed content calculation “**fd**” models are lower than values for the corresponding uniform dispersal approximation “**cha**” model. The “**cha**” model evaluated without polyethylene bounds results for the more realistic “**fl**” and “**fd**” models evaluated with 500 g polyethylene and the HEU content of the package confined to the specific content locations.

Powder, particulate, or small pieces of HEU potentially present in broken metal are capable of passing between content locations. The quantity of this material, potentially present, represents a small fraction of the total HEU broken metal content. However, the placement of a limit on content size for criticality control is not adopted as a package content loading restriction (Sect. 6.2.4). Instead, the loading limits established based on the “**cha**” model are retained, recognizing that the use of polyethylene is not addressed in “**cha**” model. Therefore, hydrogenous packing material will not be used in the containment vessel when broken metal content is present (Sect. 6.2.4, Item 7).

6.5.3 HEU Oxide

Like packages with HEU metal or broken metal, the neutron multiplication factor for an NCT array of packages with HEU product oxide decreases as a function of decreasing ^{235}U mass [parametric Cases **nciapdoxt11_1_n_24_3**, **nciapdoxt11_1_n_20_3**, **nciapdoxt11_1_n_15_3**, **nciapdoxt11_1_n_12_3**, **nciapdoxt11_1_n_11_3**, and **nciapdoxt11_1_1_10_3** through **nciapdoxt11_1_1_6_3** (Table 6.9.6-13b)]. For these NCT cases, the MOIFR is set at $1.0\text{E}-04$ such that neutronic interaction between packages of an array is maximized. Results for the parametric cases reveal the same consistent increase in the $k_{eff} + 2\sigma$ values with decreasing bulk density as observed in the single package calculation results (Sect. 6.4.3). Results for Cases **nciapdoxt11_1_n_11_3** and **nciapdoxt11_1_1_10_3** through **nciapdoxt11_1_1_6_3** demonstrate that over the range of HEU oxide bulk densities from 6.54 to 2.0 g/cm^3 , the $k_{eff} + 2\sigma$ values are below the USL of 0.925 .

Cases **nciask_1_15** through **nciask_10_15** (Appendix 6.9.6, Table 6.9.6-18) evaluate infinite arrays of packages having the 10 skull oxide compositions described in Sect. 6.4.3. The MOIFR is set at

1.0e-04 such that neutronic interaction between packages is maximized. The $k_{eff} + 2\sigma$ values, ranging from 0.656 to 0.764, are substantially below the below the USL value of 0.925, indicating that canned spacers are not required for criticality control.

The CSI is 0.0 for an infinite array of packages having product oxide content with a bulk density ≥ 2.0 g/cm³ and with a maximum of 9,682 g ²³⁵U or having skull oxide content with a maximum of 16,399 g ²³⁵U and 921 g graphite. The suitability of this determination is contingent upon satisfactory results under the HAC evaluation (Sect. 6.6.3.)

6.5.4 UNH Crystals

Unlike the HEU metal, broken metal, or oxide content, UNH crystals are soluble in water (Sect. 6.4.4). The most reactive content condition occurs at an optimum solution concentration derived from the UNH crystal loading and the volume of water flooding the containment vessel. Both flooding of the containment vessel and a reduced loading of UNH crystals going into solution is required to achieve the most reactive configuration.

Similar to packages with HEU metal, broken metal, or oxide, the neutron multiplication factor for an array of packages with UNH crystals decreases as a function of increasing MOIFR. Cases **nciaunhct11_8_24_1_1** through **nciaunhct11_8_24_1_15** for content without polyethylene and Cases **nciapunhct11_24_1** and **nciapunhct11_24_15** for content with 500 g polyethylene (Table 6.9.6-15) reveal the effect of isolating the individual array units from each other with the introduction of water above ~ 0.01 MOIFR. Array reactivity ($k_{eff} + 2\sigma = 0.721$ without polyethylene and 0.729 with polyethylene) approaches the reactivity of the water-saturated, water-reflected single-unit package ($k_{eff} + 2\sigma = 0.702$ without polyethylene and 0.708 with polyethylene).

In a series of NCT calculations (Cases **nciapunhct11_nn_3**), the $k_{eff} + 2\sigma$ values are above the USL of 0.925 for mass loadings between 8,000 and 24,000 g UNH crystals. Credit is not taken for water tightness that is demonstrated by the NCT (and HAC) tests. Therefore, mass loading is limited to 7,000 g UNH crystals. The CSI is 0.0 [10 CFR 71.59(a)(1) and 10 CFR 71.59(b)] for ES-3100 packages having a maximum of 3,297 g ²³⁵U. The suitability of this determination depends upon satisfactory results under the HAC evaluation of Sect. 6.6.4. [10 CFR 71.59(a)(2) and 10 CFR 71.59(b)]

The $k_{eff} + 2\sigma$ values are expected to range from subcritical to critical for array configurations where UNH crystals are dissolved in the water flooding the containment vessel and the containment vessel well. This requires intrusion of water into the containment vessel, dissolving of UNH crystals in the influent, and leakage of solution out of the containment vessels in each package of an array (catastrophic failure of all packages in an infinite array). Given that loss of containment is deemed not credible by merit of the 10 CFR 71.71 and 10 CFR 71.73 tests performed on the ES-3100, this accident condition is not credible.

For Cases **ncf1punhct12_nn_3**, the $k_{eff} + 2\sigma$ values are below the USL of 0.925. Given that the results for NCT and HAC (Sect. 6.6.4) are adequately subcritical, packages may be shipped under a CSI = 0.4 for packages with a maximum of 24,000 g UNH crystals. [10 CFR 71.59(a)(1) and 10 CFR 71.59(b)]. Likewise, the suitability of this determination depends upon satisfactory results under the HAC evaluation of Sect. 6.6.4.

6.6 EVALUATION OF PACKAGE ARRAYS UNDER HYPOTHETICAL ACCIDENT CONDITIONS

Except for UNH crystals, the package content is confined within the containment vessel for the HAC array evaluation of ES-3100 packages, consistent with the result of the tests specified in 10 CFR 71.73 (Hypothetical Accident Conditions). The array sizes examined in this evaluation are infinite, $13 \times 13 \times 6$, $9 \times 9 \times 4$, $7 \times 7 \times 3$, $5 \times 5 \times 2$, **ETP 16 \times 3**, and the degenerate single unit. The “N” and corresponding CSI values for arrays determined to be adequately subcritical are as follows: $N = \infty$, $CSI = 0$; ~~$N = 507$, $CSI = 0.1$~~ ; $N = 162$, $CSI = 0.4$; $N = 73$, $CSI = 0.7$; $N = 25$, $CSI = 2.0$; and $N = 24$, $CSI = 2.1$. All arrays, except the infinite array, are reflected with 30 cm (1 ft) of water. These array are nearly cubic in shape for optimum reactivity of the array, thus eliminating the need for placing criticality controls on package arrangements in terms of stack height, width, and depth of an array. The array configurations and the range of water contents (Table 6.4) evaluated bound all possible packaging arrangements and moderation conditions for HAC.

For the single damaged package, and for infinite and finite arrays of damaged packages with HEU metal, HEU oxide, or UNH crystal content, the neutron multiplication factor changes as a function of the ^{235}U mass, MOIFR, or applicable solution concentration in the same manner as in an array of undamaged packages.

6.6.1 Solid HEU Metal of Specified Geometric Shapes

For infinite and finite arrays of damaged packages with HEU metal, the neutron multiplication factor increases as a function of the ^{235}U mass and decreases as a function of MOIFR. For example, consider the ES-3100 package loaded with three convenience cans that contain a 3.24-in.-diam cylinder with 12,000 g ^{235}U for a total of 36,000 g ^{235}U . For package content without 277-4 canned spacers, the $k_{eff} + 2\sigma$ values range from 1.027 to 0.967 with increasing MOIFR in the damaged packages [Cases **hciaoct12_36_1_1** through **hciaoct12_36_1_15** (Appendix 6.9.6, Table 6.9.6-3)]. For package content with 277-4 canned spacers, the $k_{eff} + 2\sigma$ values range from 0.956 to 0.884 with increasing MOIFR in the damaged package [Cases **hciaoct12_36_2_1** through **hciaoct12_36_2_15** (Appendix 6.9.6, Table 6.9.6-3)].

The introduction of water above ~ 0.01 MOIFR shows the effect of isolating the individual array units from each other. The neutron multiplication factor approaches k_{eff} for the single, water-reflected unit at a full content-water fraction (MOIFR = 1.0). Comparison of these results with the corresponding NCT cases (Sect. 6.5.1.) indicates no significant differences. This result is as expected given that the neutron multiplication in an infinite array is independent of pitch between fissile contents but is dependent on changes in mass and moderation in the array. The changes in both the outer dimensions and the compositions of the Kaolite and 277-4 of the ES-3100 package due to HAC result in changes to the neutron multiplication factor on the order of ~ 0.001 to 0.002.

Repeated for 4.25-in.-diam cylinders (Appendix 6.9.6, Table 6.9.6-7); 2.29-in.-square bars (Table 6.9.6-5); and 1.5-in.-diam \times 2-in.-tall slugs (Table 6.9.6-9), this type of analysis for the 3.24-in.-diam cylinders demonstrates that arrays of damaged packages with restricted fissile material (^{235}U) loading remain subcritical over the entire range of water content or MOIFR. HEU bulk metal or alloy content not covered by the specified geometric shapes (cylinder, square bar, or slug contents) will be in the HEU broken metal category, and so limited.

Cases **hciaotriga_1_1_3** through **hciaotriga_1_15_3** (Appendix 6.9.6, Table 6.9.6-20) represent infinite arrays of damaged packages containing the bounding TRIGA fuel content (20 % enrichment with 45 wt % U containing 307 g ^{235}U), without 277-4 canned spacers. For these cases, the $k_{eff} + 2\sigma$ values increase from 0.218 to 0.526 as MOIFR increases. The $k_{eff} + 2\sigma = 0.526$ for Case **hciaotriga_1_15_3** is

substantially below the USL of 0.925, indicating that canned spacers are not required for criticality control. Given that the results for NCT (Sect. 6.5.2) and HAC are adequately subcritical, packages with TRIGA fuel content ≤ 921 g ^{235}U may be shipped under a $\text{CSI} = 0$.

As stated in Sect. 6.5.1, calculation results presented in Table 6.9.6-20d for an infinite array of ES-3100 packages (NCT packaging with extremely damaged TRIGA fuel content) is substantially below the USL of 0.925. Similar results are expected for an infinite array of ES-3100 packages (HAC packaging with extremely damaged TRIGA fuel content) given that changes external to the containment vessel due to the HAC do not result in an appreciable change in the neutron multiplication for the an array of packages. Therefore, the 10 CFR 71.55(e)(1) requirement that the package be adequately subcritical under HAC with the package contents in the most reactive credible configuration is satisfied.

The array results for three slug configurations presented in Table 6.9.6-9 (Appendix 6.9.6) are for five or ten slugs touching or spaced apart in a pentagonal ring (Cases **hcia5st12** and **hcia5est12**) and for seven slugs formed by a hexagonal ring of slugs with one slug in the center of the ring (**hcia70st12**). These cases are used to establish the mass loading limitations for damaged packages, which in turn limit the number of slugs in the package to less than the number required to assemble a critical configuration.

Cases **hcia5est12_1_1_8_3** through **hcia5est12_1_1_1_3** and Cases **hcia5st12_1_1_8_3** through **hcia5st12_1_1_1_3** (Appendix 6.9.6, Table 6.9.6-9) represent infinite arrays of damaged packages containing 18,277 g U without 277-4 canned spacers. Infinite array Cases **hcia70st11_2_8_3** through **hcia70st11_2_1_3** represent damaged packages containing 25,588 g U with 277-4 canned spacers while Cases **hcia5est12_2_2_8_3** through **hcia5est12_2_2_1_3** represent damaged packages containing 36,558 g U also with 277-4 canned spacers. Cases **hcf25est12_2_2_8_3** through **hcf25est12_2_2_1_3** represent a $9 \times 9 \times 4$ array of damaged packages containing 36,558 g U with 277-4 canned spacers. The $k_{\text{eff}} + 2\sigma$ values for these cases representing arrays of damaged packages are slightly less than values for the corresponding cases representing undamaged packages. (The changes in both the outer dimensions of the package and the compositions of the Kaolite and 277-4 due to HAC result in an ~ 0.001 change in the neutron multiplication factor.) Therefore, the prospective CSI values determined in the NCT evaluation (Sect. 6.5.1) for arrays of undamaged packages with slug content are controlling.

6.6.2 HEU Solid Metal of Unspecified Geometric Shapes or HEU Broken Metal

Consider the ES-3100 package loaded with three convenience cans for a total of 35,142 g ^{235}U with no canned spacers between content locations. The $k_{\text{eff}} + 2\sigma$ values range from 1.14 to 0.939 with increasing MOIFR, Cases **hciabmt12_36_1_8_1** through **hciabmt12_36_1_8_15** (Appendix 6.9.6, Table 6.9.6-11). The introduction of water above ~ 0.01 MOIFR shows the effect of isolating the individual array units from each other. Array reactivity ($k_{\text{eff}} + 2\sigma = 0.939$) approaches the reactivity of the water-saturated, water-reflected single package ($k_{\text{eff}} + 2\sigma = 0.891$, Case **hcsrbmt12_36_1_15**, Table 6.9.6-11).

Cases **hciabmt12_1_nn_mm_3** through **hciabmt12_36_nn_mm_3** model the ES-3100 with the reduced-diameter HAC package model where the enrichment of the content is varied from 60 wt % to 100 wt % ^{235}U . These array cases with $\text{MOIFR} = 1\text{e-}04$ pertain specifically to HAC packages where the neutron poison of the body weldment liner inner cavity is at 90% moisture content, but the Kaolite is dry (in the as-manufactured condition), and neither recess of the package external to the containment vessel and the interstitial space between the drums of the array contains any residual moisture. As stated before, this HAC case is more reactive than all other HAC cases where more moisture is present in the Kaolite and recesses of the package. Increasing the interspersed water between the containment vessels in the array will reduce neutronic interaction between the flooded contents to a point where the packages of the array become isolated.

Ranges of enrichment are specified in Table 6.1b (10 CFR 71.59) for identifying fissile mass loading limits for HEU broken metal. Consider specifically enrichments >95 wt % ^{235}U . The containment vessel calculations (Case **cvr3lha_36_1_8_15** versus Case **cvr3lha_36_2_8_15**, Appendix 6.9.6, Table 6.9.6-10) indicate that 277-4 canned spacers are required in this enrichment range, where the maximum evaluated mass loading of 35,142 g ^{235}U is possible. However, the fissile mass loading must be limited to 2774 g ^{235}U (Case **hciafmt12_3_2_8_3**) in order for the $k_{\text{eff}} + 2\sigma$ value ($= 0.905$) to be below the USL of 0.925. This fissile mass limit is conservative when applied to enrichments only slightly greater than 95 wt % ^{235}U . Given that the results for NCT (Sect. 6.5.2) and HAC are adequately subcritical, packages ≤ 2774 g ^{235}U and enrichment >95 wt % ^{235}U may be shipped under a $\text{CSI} = 0$.

This evaluation technique for determination of mass loading limits for enrichment intervals is repeated over the range of HEU enrichments. At HEU enrichment <60 wt % ^{235}U , the package mass loading limit is achieved, so no further delineation is required.

The loading limits for HEU solid metal of unspecified geometric shapes or HEU broken metal are summarized in Table 6.2a and are based on the array calculation performed using the uniform dispersal approximation "cha" model (Fig. 6.9.1-5d). The calculation results on which the determination is based are summarized in Table 6.1c. These loading limits were re-evaluated using the packaging fraction ("fl") and the dispersed content ("fd") calculation models.

HAC cases are documented in Table 6.9.6-11c. The reference case results based on the uniform dispersal approximation "cha" model are highlighted. The corresponding cases for the packaging fraction ("fl") and for the dispersed content ("fd") calculation models are given in the rows below the reference case.

The loading limits for HEU solid metal of unspecified geometric shapes or for HEU broken metal are summarized in Table 6.2a based on array calculations performed using the uniform dispersal approximation "cha" model (Fig. 6.9.1-5d). The calculation results on which the determination of the loading limits is based are summarized in Table 6.1c.

As discussed in Sect. 6.5.2, criticality calculations with the "cha" model for a packing fraction of ~ 0.59 bound similar cases at the lower packing fractions. The "cha" model is characteristic of the situation where the dimensions of the broken metal pieces are sufficiently small to allow for HEU to pass between void space formed between the inner wall of the containment vessel and the exterior wall of each canned spacer.

As shown in Fig. 6.9.3.1-3, HEU broken metal content typically consists of irregular pieces, sufficiently large (0.5 in. to several inches on a side), that will not pass between the 277-4 canned spacer locations. The packing fraction calculation model "fl" and the dispersed content calculation model "fd" better represent broken metal content which does not pass between the canned spacer locations.

HAC cases are documented in Table 6.9.6-11c. The reference case results based on the uniform dispersal approximation "cha" model are highlighted. The corresponding cases for the packaging fraction ("fl") and for the dispersed content ("fd") calculation models are given in the rows below the reference case.

An increase of ~ 0.08 in the $k_{\text{eff}} + 2\sigma$ values is observed as the packing fraction is reduced and more water is homogenized with the fissile material (i.e., Cases **hciafmtf111_1_6_4_5** through **hciafmtf111_1_2_4_5**, Table 6.9.6-11c). As the packing fraction is reduced and the volume of the content location is increased, moderation of the fissile material increases. A considerable increase of ~ 0.22 in the $k_{\text{eff}} + 2\sigma$ values is observed when fissile material in the upper can location is

homogenized with water in the upper content location and dispersed over that region (i.e., Case **hciapbmtfl11_1_6_4_5** vs Case **hciapbmtfd11_1_6_4_5**, Table 6.9.6-11c). Nevertheless, the $k_{eff} + 2\sigma$ values for the packaging fraction “**fl**” and dispersed content calculation “**fd**” models are lower than values for the corresponding uniform dispersal approximation “**cha**” model. The “**cha**” model evaluated without polyethylene bounds results for the more realistic “**fl**” and “**fd**” models evaluated with 500 g polyethylene and the HEU content of the package confined to the specific content locations.

Powder, particulate, or small pieces of HEU potentially present in broken metal are capable of passing between content locations. The quantity of this material, potentially present, represents a small fraction of the total HEU broken metal content. However, the placement of a limit on content size for criticality control is not adopted as a package content loading restriction (Sect. 6.2.4). Instead, the loading limits established based on the “**cha**” model are retained, recognizing that the use of polyethylene is not addressed in “**cha**” model. Therefore, hydrogenous packing material will not be used in the containment vessel when broken metal content is present (Sect. 6.2.4, Item 7).

6.6.3 HEU Oxide

Like packages with HEU metal or broken metal, the neutron multiplication factor for an array of HAC packages with HEU product oxide decreases as a function of decreasing ^{235}U mass [parametric Cases **hciapdopt11_1_n_24_3**, **hciapdopt11_1_n_20_3**, **hciapdopt11_1_n_15_3**, **hciapdopt11_1_n_12_3**, **hciapdopt11_1_n_11_3**, and **hciapdopt11_1_1_10_3** through **hciapdopt11_1_1_6_3** (Table 6.9.6-13b)]. For these HAC cases, the MOIFR is set at 1.0E-04 such that neutronic interaction between packages of an array is maximized. Results for the parametric cases reveal the same consistent increase in the $k_{eff} + 2\sigma$ values with decreasing bulk density as observed in the single package calculation results (Sect. 6.4.3). Results for Cases **hciapdopt11_1_n_11_3** and **hciapdopt11_1_1_10_3** through **hciapdopt11_1_1_6_3** demonstrate that over the range of HEU oxide bulk densities from 6.54 to 2.0 g/cm³, the $k_{eff} + 2\sigma$ values are below the USL of 0.925. Given that the results for NCT (Sect. 6.5.3) and HAC are adequately subcritical, packages may be shipped under a CSI = 0.0 for an infinite array of packages having product oxide with a maximum of 9,682 g ^{235}U .

Cases **hciask_1_15** through **hciask_10_15** (Appendix 6.9.6, Table 6.9.6-18b) evaluate infinite arrays of damaged packages having the 10 skull oxide compositions described in Sect. 6.4.3. The differences between the HAC case results and the NCT case results are not statistically significant. The $k_{eff} + 2\sigma$ values, ranging from 0.658 to 0.767, are substantially below the USL value of 0.925. Given that the results for NCT (Sect. 6.5.3) and HAC are adequately subcritical, packages may be shipped under a CSI = 0.0 for an infinite array of packages having skull oxide content with a maximum of 16,399 g ^{235}U and 921 g graphite.

6.6.4 UNH Crystals

Unlike the HEU metal, broken metal, or oxide content, UNH crystals are soluble in water (Sect. 6.4.4). The most reactive content condition occurs at an optimum solution concentration derived from the UNH crystal loading and the volume of water flooding the containment vessel. Both flooding of the containment vessel and a reduced loading of UNH crystals going into solution is required to achieve the most reactive configuration.

Similar to packages with HEU metal, broken metal, or oxide, the neutron multiplication factor for an array of damaged packages with UNH crystals decreases as a function of increasing MOIFR. Cases **hciaunhct12_8_24_1_1** through **hciaunhct12_8_24_1_15** for content without polyethylene and Cases **hciaunhct12_24_1** and **hciaunhct12_24_15** for content with 500 g polyethylene (Table 6.9.6-15) reveal the effect of isolating the individual array units from each other with the

introduction of water above ~ 0.01 MOIFR. Array reactivity ($k_{eff} + 2\sigma = 0.729$ without polyethylene and 0.733 with polyethylene) approaches the reactivity of the water-saturated, water-reflected unit single package ($k_{eff} + 2\sigma = 0.704$ without polyethylene and 0.711 with polyethylene).

In a series of HAC calculations (Cases **hciapunhct11_nm_3**), the calculated $k_{eff} + 2\sigma$ values are below the USL of 0.925 for loading with $< 8,000$ g UNH crystals. Given that the results for NCT (Sect. 6.5.4) and HAC are adequately subcritical, the CSI is 0.0 [10 CFR 71.59(a)(2) and 10 CFR 71.59(b)] for packages having a maximum of 3,297 g ^{235}U .

The $k_{eff} + 2\sigma$ values are expected to range from subcritical to critical for array configurations where UNH crystals are dissolved in the water flooding the containment vessel and the containment vessel well. This requires intrusion of water into the containment vessel, dissolving of UNH crystals in the influent, and leakage of solution out of the containment vessels in each package of an array. The leakage out of the containment vessel of content moderated "to such an extent as to cause maximum reactivity consistent with the physical and chemical form of material" is not considered credible HAC based on results for tests specified in 10 CFR 71.73.

In a series of HAC calculations (Cases **hcf2punhct12_nm_3**), the calculated $k_{eff} + 2\sigma$ values are below the USL of 0.925. Given that the results for NCT (Sect. 6.5.4) and HAC are adequately subcritical, packages may be shipped under a CSI = 0.4 for packages with a maximum of 24,000 g UNH crystals.

6.7 FISSILE MATERIAL PACKAGES FOR AIR TRANSPORT

A series of calculations are performed for determining the most reactive configuration of the content and surrounding packaging material in an ES-3100 package that undergoes catastrophic destruction. Fissile content mass loadings that remain under the USL for these catastrophic events are identified. Subcriticality is demonstrated after due consideration of such aspects as the efficiency of moderator, loss of neutron absorbers, rearrangement of packaging components and contents, geometry changes and temperature effects. The seven calculation models used in this evaluation are described in Sect 6.3.1.4. Key model dimensions and parameters are tabulated in Tables 6.9.6-21 through 6.9.6-23, Appendix 6.9.6.

6.7.1 Results for Solid HEU, One Piece per Convenience Can

Cases **atdmr_10_8** through **atdmr_7_1** (Table 6.9.6-21, Appendix 6.9.6) pertain to Model 1 (Fig. 6.11, Section 6.3.1.4). HEU solid or broken metal of three convenience cans is homogenized with 513 g of polyethylene, representing the potential use of hydrogenous packing materials in the ES-3100. The fissile core is configured into a spherical shape with an exterior 20 cm water reflector. As shown in

Cases **athmpkmr_6_1_1_11** through **athmpwskr_1_6_1_1** (Table 6.9.6-23, Appendix 6.9.6) pertain to Model 6 (Fig. 6.16, Section 6.3.1.4), where fissile material from the homogenized core of Model 4 forms a shell external to the core. Cases **athmpkmr_6_1_1_11** through **athmpkmr_6_1_1_1** represent 3 kg ^{235}U in the core and 0.5 kg ^{235}U in the shell (17.5 kg total HEU at 20% enrichment) with the water content of the Kaolite ranging from the water-saturated to the dry condition. In the subsequent series of cases, the $k_{\text{eff}} + 2\sigma$ values decrease as HEU is moved from the core to the shell in 2.5 kg increments. Although the total HEU of 17.5 kg greatly exceeds the 3.5 kg limit identified in the evaluation of Model 5, all $k_{\text{eff}} + 2\sigma$ values are adequately below the USL of 0.925.

As stated previously, uranium alloy is conservatively assessed when the aluminum or molybdenum constituents are modeled as ^{235}U . Thus, limits established for HEU metal apply to the uranium alloys of aluminum or molybdenum.

6.7.4 Conclusions

Given that the results for catastrophic damage are adequately subcritical, ES-3100 packages may be shipped via air transport with:

- Solid or broken HEU metal or U-Al alloy with up to 700 g ^{235}U ,
- 3 fuel sections ("meats") of UZrH_x per loaded convenience can and up to 3 loaded cans per package where the ^{235}U does not exceed 716 g at 20% enrichment or 408 g ^{235}U at 70%,
- ~15 inch long clad fuel rods, each rod derived from a single TRIGA fuel element, and where per package ^{235}U does not exceed 716 g at 20% enrichment or 408 g ^{235}U at 70%, or
- oxides of U_3O_8 , $\text{U}_3\text{O}_8\text{-Al}$, UO_2 , and $\text{UO}_2\text{-Mg}$ where the per package ^{235}U content does not exceed 716 g at enrichments less than or equal to 20% or 408 g ^{235}U at enrichments greater than 20%.

6.8 BENCHMARK EXPERIMENTS

6.8.1 Applicability of Benchmark Experiments

The criticality validation is specific to uranium, plutonium, and uranium-233 systems encompassing a substantial subset of the database used to prepare the Organization for Economic Cooperation and Development (OECD) Handbook, Volumes I–VI. The benchmark specifications are intended for use by criticality safety engineers to validate the application of criticality calculation techniques such as SCALE 4.4a. Example calculations presented in the handbook do not constitute a validation of the codes or cross-section data sets by themselves, but the Handbook information can be and has been used to validate SCALE 4.4a by competent nuclear criticality safety persons.

The data from the benchmark experiments involving uranium represent a sufficiently wide range of enrichments and physical and chemical forms to cover many existing or presently planned activities for Y-12. These include enriched uranium with ^{235}U only and natural and depleted uranium, as well as highly enriched uranium, intermediate enriched uranium, and low enriched uranium. Data analyzed from critical experiments in this validation include systems having fast, intermediate, and thermal neutron energy spectra, and they include materials in various physical and chemical forms such as uranium metals, solutions, and oxide compounds. With the benchmark experiments that are directly applicable to

uranium systems, there is a high level of confidence that the calculated results presented in this evaluation are sufficiently accurate to establish the safety of the package under both NCT and HAC. This conclusion is based on the validation of the code and cross-section library described in Sect. 6.3.3.

6.8.2 Details of Benchmark Calculations

The validation of CSAS25 control module of SCALE 4.4a with the 238-group ENDF/B-V cross-section library is documented in Y/DD-896/R1 and Y/DD-972R1 (Appendix 6.9.8). Y/DD-896/R1 addresses the establishment of bias, bias trends, and uncertainty associated with the use of SCALE 4.4a for performance of criticality calculations. This evaluation is directed at uranium systems consisting of fissile and fissionable material in metallic, solution, and other physical forms, as well as plutonium and ^{233}U systems, as described in the OECD Handbook. [NEA/NSC/DOC(95)03] The focus is on comparison of k_{eff} with the associated experimental results for establishment of bias, bias trends, and uncertainty as a final step. Compiled data for 1217 critical experiments are used as the basis for the calculation models. The calculated results from SCALE 4.4a using the 238-group ENDF/B-V cross-section library have been compared with reported results for the benchmark experiments. Comparison of results demonstrates that SCALE 4.4a run on the SAE HP J-5600 unclassified workstation (CMODB) produces the same results within the statistical uncertainty of the Monte Carlo calculations as reported by the OECD for the experiments.

Y/DD-972R1 (Appendix 6.9.8) addresses determining USL and for incorporating uncertainty and margin into this USL. Y/DD-972R1 establishes subcritical limits determined through an evaluation of statistical parameters of calculation results for critical experiments. The correlating parameters (i.e., mass, enrichment, geometry, absorption, moderation, reflection) and values for applying additional margin to the subcritical limits are application dependent. The determination of correlating parameters and additional margin is an integral part of the process analysis for a particular application. For the critical experiment results, no correlation between calculation results and neutron energy causing fission was found. As such, this document does not specify "final" USL values as has been done in the past.

6.8.3 Bias Determination

The USL is based on the non-parametric statistics-based lower tolerance limit (LTL) for greater than 0.99/99% where there is a probability of greater than 0.99 that 99% of the population is greater than a specified result, reduced by additional margin. From Table 1 of Y/DD-972R1 (Appendix 6.9.8), the LTL combining bias and bias uncertainty is 0.975 for uranium systems, including HEU metal, ~~indicating a bias value of 0.025~~. Tables 4.2, 4.3, and 4.4 of Y/DD-896/R1 (Appendix 6.9.8) list the maximum (positive) and minimum (negative) biases for HEU (metal, compound, solution), IEU (metal, compound) and LEU (compound, solution) systems. Since the positive bias is conservatively treated as a "zero" bias in the validation analysis, the negative bias is applied to determine the USL for the systems. The minimum bias for the HEU, IEU, and LEU systems is given as -0.0203, -0.0055 and -0.0247, respectively. The global minimum bias for these systems [-0.0247 (conservatively rounded to -0.025)] is applied to all uranium enrichments. Ordinarily, the USL would be 0.955 where an additional margin of subcriticality of 0.02 is subtracted from the LTL of 0.975. However, NUREG/CR-5661 provides guidance that the USL should be established with a minimum margin of subcriticality of 0.05. Thus, the USL is equal to 0.95 plus the minimum bias (-0.025), giving a value of 0.925.

Calculation model for solid HEU metal, slugs. Figure 6.9.1-4 depicts the wire-mesh view of a pentagonal ring configuration of the 1.5-in.-diam \times 2.0-in.-tall slugs inside the containment vessel. The axial centerline of each slug is located 1.27598 in. from the origin of the pentagon such that a tight fitting configuration of slugs is modeled (i.e., there are no gaps between adjacent slugs). The slug content model contains two rings of the 1.5-in.-diam \times 2.0-in.-tall slugs per convenience can and the 277-4 canned spacers between the convenience cans locations. The interstitial water inside the containment vessel has been removed for illustration purposes. Figure 6.9.1-4b depicts typical slug configurations that were evaluated.

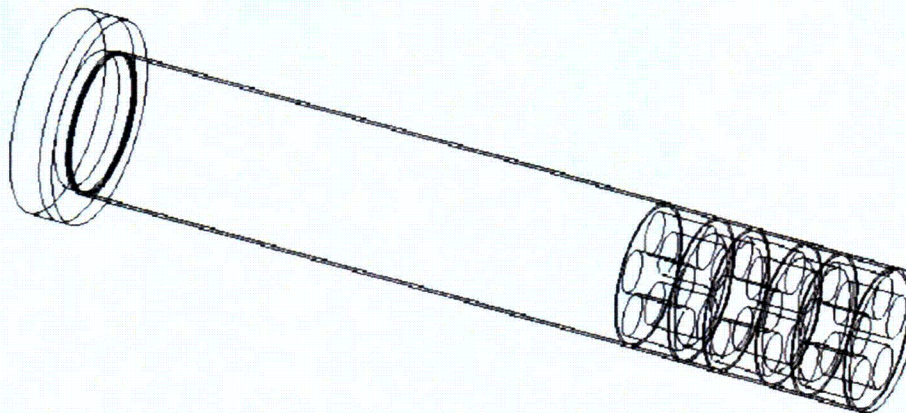
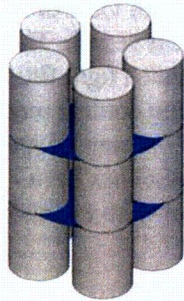


Fig. 6.9.1-4. Containment vessel containing the 1.5-in.-diam \times 2.0-in.-tall slugs in a pentagonal ring configuration with 0.0-cm spacing between slugs and 1.4-in.-thick 277-4 canned spacers.

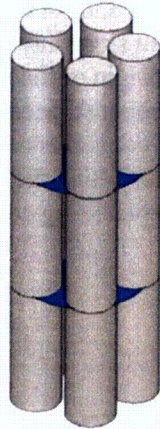
A 1.5-in.-diam \times 2.0-in.-tall slug was modeled with a maximum tolerance of 1/16 in. applied to both the radius and height. The resulting dimensions are 1.984375 cm in radius and 5.23875 cm in height; the calculated volume of a single slug is 64.80746 cm³. For 100% enriched uranium (density = 18.81109 g/cm³), the calculated mass of 15 slugs is 18,286.5 g. Subsequently, the radius of each slug was reduced by 0.0005 cm thus eliminating a geometry intersection error in KENO V.a which occurs when the hole option is used to place slugs into an encompassing piece of the geometry unit. In the case of a pentagonal ring with spaced-apart slugs (Case **cvr5est11_1_1**, Fig. 6.9.1-4b), the calculated volume reported for 15 slugs in KENO V.a is 971.622 cm³ and the corresponding mass is 18277.3 g or 1,218.5 g per slug. This reduction in mass of 0.6333 g per slug is insignificant when considering the mass of a slug is nominally 1,089 g.

The maximum tolerance slug was also used in other slug geometry configurations, such as, “cvr5s”, “cvr6e0s”, “cvr6s”, “cvr70s”, “cvr6e4s”, and “cvr73s” orientations shown in Fig. 6.9.1-4b. For the pentagonal geometry configuration with slugs stacked two high in a ring (Case **cvr5est11_1_2** or **cvr5st11_1_2**), the model volume and mass of the slugs are twice the values of the single ring (Case **cvr5est11_1_1** or **cvr5st11_1_1**). For a pentagonal geometry configuration with a central slug (“cvr6e0s”) and the hexagonal geometry configuration (“cvr6”), the calculated volume reported in KENO V.a is 1,165.95 cm³ and the corresponding mass is 21,932.7 g. For a hexagonal geometry configuration with a central slug (“cvr70s”), the calculated volume reported in KENO V.a is 1,360.27 cm³ and the corresponding mass is 25,588.2 g. For the compact ten-slug-per-can configurations (“cvr5est”, “cvr5st”, “cvr6e4s”, and “cvr73s”), the calculated volume reported in KENO V.a is 1,943.24 cm³, and the corresponding mass is 36,554.6 g.

Several slug arrangements were evaluated for demonstrating that the most conservative arrangement of slugs has been analyzed. Figure 6.9.1-4c depicts radial section views of the containment vessel showing the slugs (pink) in relation to the footprint (blue) for a 4.25-in.-diam (5.3975-cm) convenience can. Cases **cvr5st11_1_1**, **cvr5est11_1_1**, **cvr5e0st11_1_1**, **cvr5u0st11_1_1**, and **cvr5l0st11_1_1** depict different arrangements with five slugs per convenience can, three cans per package. Cases **cvr6e0st11_1_1** and **cvr6st11_1_1** depict arrangements with six slugs per convenience can, and Case **cvr70st11_1_1** depicts seven slugs per convenience can. (Considerable deformation of a 4.25-in.-diam convenience can wall is required to achieve all but the simple pentagonal-ring arrangement of slugs.) The 277-4 canned spacers are not present in these calculation models.



cvc5est11_1_1
18,277 g ²³⁵U
no canned spacers



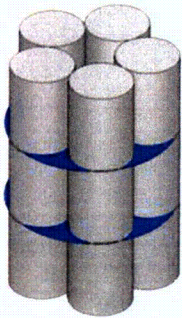
cvc5est11_1_2
36,555 g ²³⁵U
no canned spacers



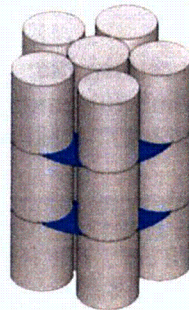
cvc5est11_2_1
18,277 g ²³⁵U
canned spacers



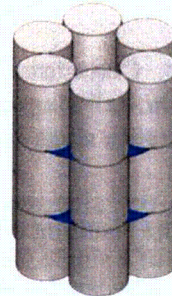
cvc5est11_2_2
36,555 g ²³⁵U
canned spacers



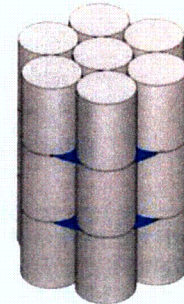
cvc5st11_1_1
18,277 g ²³⁵U
no canned spacers



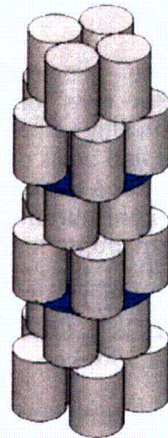
cvc6e0st11_1
21,933 g ²³⁵U
no canned spacers



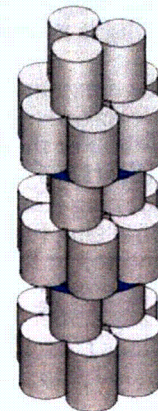
cvc6st11_1_1
21,933 g ²³⁵U
no canned spacers



cvc70st11_1
25,588 g ²³⁵U
no canned spacers



cvc6e4st11_1
36,555 g ²³⁵U
no canned spacers



cvc73st11_1
36,555 g ²³⁵U
no canned spacers

Fig. 6.9.1-4b. Isometric views for typical slug configurations. Blue marker depicted for configurations without 1.4-in.-thick 277-4 canned spacers.

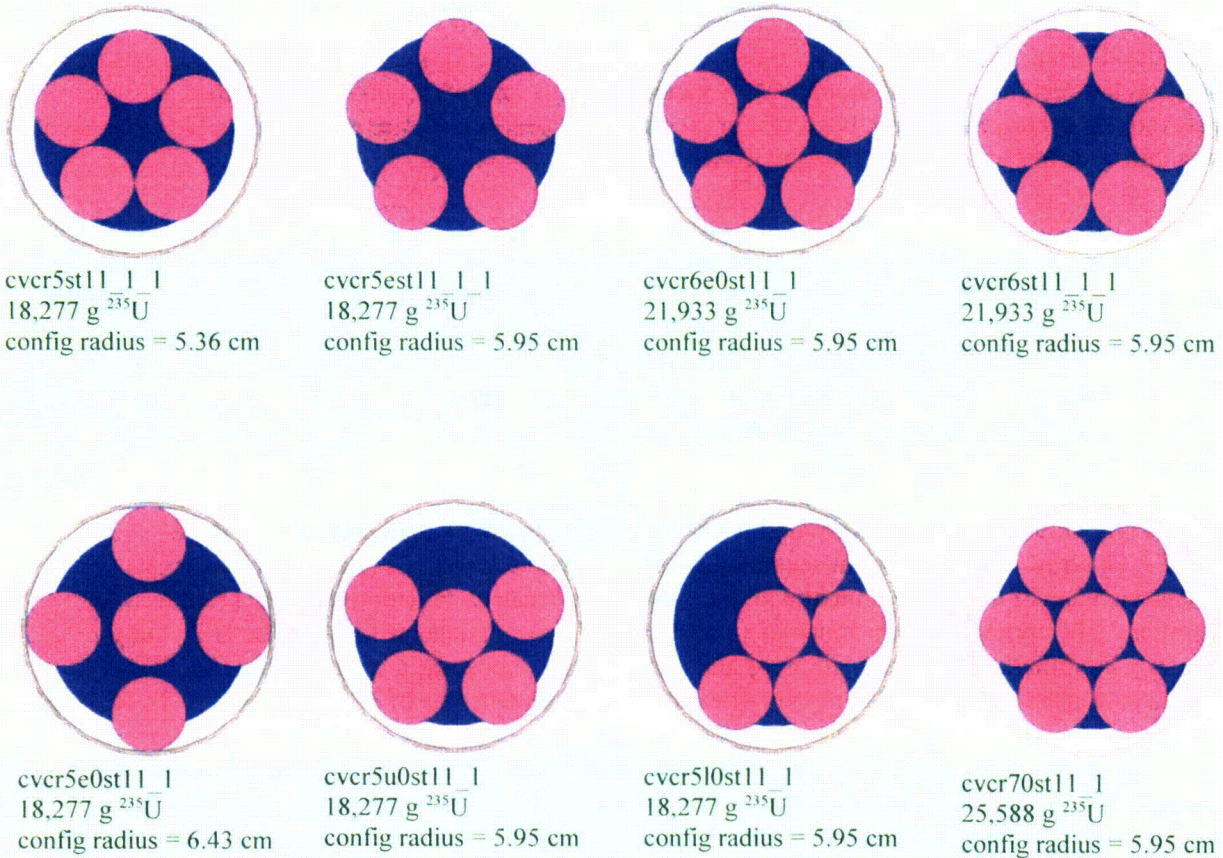


Fig. 6.9.1-4c. Plan view of slug configurations in the confines of the containment vessel. Blue marker depicts 4.25-in.-diam wall of the convenience can.

Calculation models for solid HEU metal of unspecified geometric shapes characterized as broken metal. The intended use of the “broken metal” category is for shipment of solid HEU metal of unspecified geometric shape characterized as broken metal, packed in 4.25-in.-diam convenience cans where the packing fraction would not exceed 0.59. The packing fraction is a parameter which characterizes the volume that broken metal occupies. A typical broken metal content is depicted in Fig. 6.9.3.1-3 where the packing fraction for content in a convenience can ranges from 0.2 to ~0.6.

In the criticality evaluation of broken metal, convenience cans are not credited for containing the content nor for maintaining spacing between the 277-4 canned spacers. Consequently, the shape and size of the broken metal pieces establishes the separation between canned spacers which in turn determines the size of the HEU content locations inside the containment vessel. Given the irregular shape of broken metal, the packing fraction is the parameter which quantifies the volume of space that the broken metal occupies. The use of a large packing fraction (~0.6) results in minimum separation between canned spacers which minimizes the size of the lower and middle content locations and maximizes the size of the upper content location. Reactivity of the containment vessel is driven by the oversized upper content location. Conversely, the use of a small packing fraction (~0.2) February 16, 2009 results in greater separation between the canned spacers which increases the size of the lower and middle content locations while reducing the size of the upper content location. Reactivity of the containment vessel decreases accordingly.

The “**sqa**”, “**lha**”, and “**cha**” calculation models are devised for evaluating broken metal in the idealized forms described in the following paragraphs. The heights of the lower can locations and separation between the first and second 277-4 canned spacers inside the containment vessel are conservatively established on the basis that broken metal is confined within a rectangular lattice formed by the unit cells of fissile material having a packing fraction of ~0.59.

In the “**sqa**” model for HEU broken metal, a uniform-size metal cube is contained inside a unit cell of content. The unit cells are configured into arrays with one array for each can location inside the containment vessel. HEU metal cubes ranging in size from 1.0 to 0.25 in. are correspondingly arranged into 3×3 , 6×6 , or 12×12 configurations with N layers stacked vertically. A rectangular lattice of unit cells is defined by a square prism circumscribed by the wall of the containment vessel with an inner diameter of 5.06 in. (12.8524 cm). The width and depth of the square base is 3.57796 in. (9.08802 cm). The height of the lattice is determined by both the size of a cube and the number of layers of cubes required for a given HEU mass loading.

Figure 6.9.1-5 depicts a wire mesh view of the containment vessel and lid with three $12 \times 12 \times 18$ arrays of HEU content separated by 277-4 canned spacers. Figure 6.9.1-5b depicts an isometric view of this same content with the **evaluation** water surrounding the HEU removed for illustration. The corner unit cells touch the inside wall of the containment vessel. The HEU cubes are centered within the individual unit cells and uniform spacing between cubes is modeled. The 277-4 canned spacers are modeled as cylindrical disks with dimensions of 4.13-in. diam \times 1.37-in. height.

Uranium mass is reduced in the calculation model by removing one or more cubes from the array and filling these vacancies with water. The location of the 277-4 canned spacers between the arrays of cubes decreases as complete layers of cubes are removed from each array. The volume of the containment vessel above the top layer of the top array of cubes is filled with full-density water.

In the “**lha**” model of HEU broken metal, the metal cubes of the “**sqa**” model are homogeneously mixed with **evaluation** water within the square prism of the “**sqa**” model. Figure 6.9.1-5c depicts an isometric view of the “**lha**” model. The boundaries of each square prism shown in the figure are defined by the $12 \times 12 \times 18$ array of unit cells of the explicit “**sqa**” model. Each prism contains the same mass of HEU and **evaluation** water that the respective explicit cube model contains. The volume outside the prisms and the canned spacers is filled with full density water.

In the “**cha**” model of HEU broken metal, the metal cubes of the “**sqa**” model are homogeneously mixed with the **evaluation** water within the free volume of the containment vessel. Figure 6.9.1-5d depicts an isometric view of the “**cha**” model. The 277-4 canned spacers are positioned for similarity with the “**sqa**” and “**lha**” models using the height of the prism, defined in this case by the $12 \times 12 \times 18$ array of unit cells of the explicit “**sqa**” model. The mass of HEU and **evaluation** water of the explicit “**sqa**” model is preserved.

Once the locations of the canned spacers in the containment vessel are established based on the height of the square prism, the HEU broken metal and evaluation water inside the containment vessel are homogenized over the internal volume of the 12.8524-cm-diam containment vessel not being occupied by the canned spacers. The homogenization of fissile material with moderator to represent discrete solid HEU metal of unspecified geometric shape characterized as broken metal is unquestionably bounding only when the overall volume (and shape) containing HEU and interstitial moderator between the pieces of HEU is preserved in the approximation model.

Table 6.9.1.1 provides details of the calculation models used to establish the mass loading limits identified in Table 6.2a for surface-only modes of transportation. The table provides exact dimensions of the fissile material used in the analyses; the mass of fissile material, enrichment, and density of the fissile material used in the analysis; moderating properties of materials inside the containment vessel (water, hydrogenous packing material, represented by polyethylene, etc.), moderator density and h/x ratios; and arrangement of the fissile material including amount of spacing (if any) between the fissile material and/or 277-4 canned spacers. In the creation of a generalized geometry model for treatment of 277-4 canned spacers, the use of a non-zero thickness spacer was required by KENO V.a. An insignificant thickness of 0.0001 cm was used for representing this imaginary region.

Table 6.9.1.1. Details of calculation models used to establish mass loading limits for surface-only modes of transportation identified in Table 6.2a

Case	Dimensions (cm)	Enrichment (wt. % ²³⁵ U)	Density (g/cm ³)
<i>Cylinders (d ≤ 3.24 in.)</i>			
nciacyt11_18_1_3	r = 4.1148 cm h = 5.99639 cm	100	18.81109
The moderator is full density water (0.9982 g/cm ³) surrounding three stacked cylindrical contents. The contents have an overall stack height of 17.99171 cm (7.08335 in.). No polyethylene was used in this model. Each cylindrical content is separated by a 0.0001 cm 277-4 canned spacer and 0.0012 cm of moderating material. The bottom cylinder has a 0.0005 cm gap between it and the bottom of the containment vessel. The contents sit in the exact center on the bottom of the CV. Therefore, the cylinder content has 2.3114 cm of moderating material around each side and 60.74779 cm of moderating material above. The modeled material masses are: 18 kg ²³⁵ U, 9.2418 kg H ₂ O, resulting in an h/x ratio of ~13.40.			
nciacyt11_30_2_3	r = 4.11480 cm h = 9.99399 cm	100	18.81109
The moderator is full density water (0.9982 g/cm ³) surrounding three stacked cylindrical contents separated by 277-4 canned spacers between each cylindrical content. The contents (uranium and spacers) have an overall stack height of 37.09657 cm (14.60495 in.). No polyethylene was used in this model. Each cylindrical content is separated by a 3.5561 cm spacer and 0.0012 cm of moderating material. The bottom cylinder has a 0.0005 cm gap between it and the bottom of the containment vessel. The contents sit in the exact center on the bottom of the CV. Therefore, the cylinder content has 2.3114 cm of moderating material around each side and 41.64293 cm of moderating material above. The modeled material masses are: 30 kg ²³⁵ U, 7.9915 kg H ₂ O, resulting in an h/x ratio of ~6.95.			
<i>Cylinders (3.24 in. < d ≤ 4.25 in.)</i>			
nciacyt11_15_1_3	r = 5.39750 cm h = 2.90416 cm	100	18.81109
The moderator is full density water (0.9982 g/cm ³) surrounding three stacked cylindrical contents separated by 277-4 canned spacers. The contents have an overall stack height of 8.71508 cm (3.43133 in.). No polyethylene was used in this model. Each cylindrical content is separated by a 0.0001 cm spacer and 0.0012 cm of moderating material. The bottom cylinder has a 0.0005 cm gap between it and the bottom of the containment vessel. The contents sit in the exact center on the bottom of the CV. Therefore, the cylinder content has 1.0287 cm of moderating material around each side and 70.02442 cm of moderating material above. The modeled material masses are: 15 kg ²³⁵ U, 9.4010 kg H ₂ O, resulting in an h/x ratio of ~16.36.			

Table 6.9.1.1. Details of calculation models used to establish mass loading limits for surface-only modes of transportation identified in Table 6.2a

Case	Dimensions (cm)	Enrichment (wt. % ²³⁵ U)	Density (g/cm ³)
nciacyct11_25_2_3	r = 5.39750 cm h = 4.84031 cm	100	18.81109
The moderator is full density water (0.9982 g/cm ³) surrounding three stacked cylindrical contents separated by 277-4 canned spacers. The contents have an overall stack height of 21.63433 cm (8.517453 in.). No polyethylene was used in this model. Each cylindrical content is separated by a 3.5561 cm spacer and 0.0012 cm of moderating material. The bottom cylinder has a 0.0005 cm gap between it and the bottom of the containment vessel. The contents sit in the exact center on the bottom of the CV. Therefore, the cylinder content has 1.0287 cm of moderating material around each side and 57.10417 cm of moderating material above. The modeled material masses are: 25 kg ²³⁵ U, 8.2568 kg H ₂ O, resulting in an h/x ratio of ~8.62.			
<i>Bars</i>			
hciasqt12_30_1_3	x = 5.81920 cm y = 5.81920 cm z = 15.69855 cm	100	18.81109
The moderator is full density water (0.9982 g/cm ³) surrounding three stacked square or cuboid contents separated by 277-4 canned spacers. The contents have an overall stack height of 47.09825 cm (18.54262 in.). No polyethylene was used in this model. Each cuboid content is separated by a 0.0001 cm spacer and 0.0012 cm of moderating material. The bottom cuboid has a 0.0005 cm gap between it and the bottom of the containment vessel. The contents sit in the exact center on the bottom of the CV. Therefore, the cuboid content is surrounded by moderating material ranging from 3.6166 to 2.4144 cm (center to outer edge) and 31.64125 cm of moderating material above. The modeled material masses are: 30 kg ²³⁵ U, 8.6050 kg H ₂ O, resulting in an h/x ratio of ~7.49.			
nciasqt11_36_2_3	x = 5.81920 cm y = 5.81920 cm z = 18.83826 cm	100	18.81109
The moderator is full density water (0.9982 g/cm ³) surrounding three stacked square or cuboid contents separated by 277-4 canned spacers. The contents have an overall stack height of 63.62938 cm (25.05094 in.). No polyethylene was used in this model. Each cuboid content is separated by a 3.5561 cm spacer and 0.0012 cm of moderating material. The bottom cuboid has a 0.0005 cm gap between it and the bottom of the containment vessel. Therefore, the cuboid content is surrounded by moderating material ranging from 3.6166 to 2.4144 cm (center to outer edge) and 15.11012 cm of moderating material above. The modeled material masses are: 36 kg ²³⁵ U, 7.6731 kg H ₂ O, resulting in an h/x ratio of ~5.56.			
<i>Slugs (enr. ≤ 95%—no can spacers)</i>			
ncia5st11_1_1_7_3	r = 1.983875 cm h = 5.23875 cm	95	18.82298
The moderator is full density water (0.9982 g/cm ³) surrounding three stacked pentagonal rings of slug content separated by 277-4 canned spacers. (Slugs are inserted into the cylindrical geometry segment of the containment vessel using the hole option.) The contents have an overall stack height of 15.71885 cm (6.18852 in.). No polyethylene is used in this model. Each ring is separated by a 0.0001 cm spacer and 0.0012 cm of moderating material. The bottom ring of slugs has a 0.0005 cm gap between it and the bottom of the containment vessel. Above the stack of slugs is 63.02065 cm of moderating material. The modeled material masses are: 18.288 kg U (17.374 kg ²³⁵ U), 9.2269 kg H ₂ O, resulting in an h/x ratio of ~13.86. The loading arrangement of slugs is depicted in Fig. 6.9.1-4b for the Case cvcr5st11_1_1 .			

Table 6.9.1.1. Details of calculation models used to establish mass loading limits for surface-only modes of transportation identified in Table 6.2a

Case	Dimensions (cm)	Enrichment (wt. % ²³⁵ U)	Density (g/cm ³)
<i>Slugs (80% < enr. ≤ 95%—with can spacers)</i>			
hcia70st12_2_7_3	r = 1.983875 cm h = 5.23875 cm	95	18.82298
The moderator is full density water (0.9982 g/cm ³) surrounding three stacked rings of slugs, each ring with a central slug surrounded by slugs in a hexagonal pattern. (Slugs are inserted into the cylindrical geometry segment of the containment vessel using the hole option.) Each ring is separated by a 277-4 canned spacer. The contents (uranium and spacers) have an overall stack height of 22.83085 cm (8.98852 in.). No polyethylene was used in this model. Each ring is separated by a 3.5561 cm spacer and 0.0012 cm of moderating material. The bottom ring has a 0.0005 cm gap between it and the bottom of the containment vessel. The stack of slugs has 55.90865 cm of moderating material above. The modeled material masses are: 25.604 kg U (24.324 kg ²³⁵ U), 8.2253 kg H ₂ O, resulting in an h/x ratio of ~8.83. The loading arrangement of slugs is similar to that depicted in Fig. 6.9.1-4b for the Case cvcr70st11_1 except that the canned spacers are present.			
ncf15est11_2_2_7_3	r = 1.983875 cm h = 5.23875 cm	95	18.82298
The moderator is full density water (0.9982 g/cm ³) surrounding three rings of double stacked slugs, each ring separated by a 277-4 canned spacer. (Slugs are inserted into the cylindrical geometry segment of the containment vessel using the hole option.) The contents (uranium and spacers) have an overall stack height of 22.83085 cm (8.98852 in.). No polyethylene was used in this model. Each ring is separated by a 3.5561 cm spacer and 0.0012 cm of moderating material. The bottom ring has a 0.0005 cm gap between it and the bottom of the containment vessel. The stack of slugs has 55.90865 cm of moderating material above. The modeled material masses are: 36.578 kg U (34.749 kg ²³⁵ U), 7.6434 kg H ₂ O, resulting in an h/x ratio of ~5.74. The loading arrangement of slugs is depicted in Fig. 6.9.1-4b for the Case cvcr5est11_2_2 .			
<i>Slugs (enr. ≤ 80%—with can spacers)</i>			
hcia5est12_2_2_5_3	r = 1.983875 cm h = 5.23875 cm	80	18.85873
The moderator is full density water (0.9982 g/cm ³) surrounding three rings of double stacked slugs, each ring separated by a 277-4 canned spacer. (Slugs are inserted into the cylindrical geometry segment of the containment vessel using the hole option.) The contents (uranium and spacers) have an overall stack height of 22.83085 cm (8.98852 in.). No polyethylene was used in this model. Each ring is separated by a 3.5561 cm spacer and 0.0012 cm of moderating material. The bottom ring has a 0.0005 cm gap between it and the bottom of the containment vessel. The stack of slugs has 55.90865 cm of moderating material above. The modeled material masses are: 36.647 kg U (29.318 kg ²³⁵ U), 7.6434 kg H ₂ O, resulting in an h/x ratio of ~6.80. The loading arrangement of slugs is depicted in Fig. 6.9.1-4b for the Case cvcr5est11_2_2 .			
ncf15est11_2_2_5_3	r = 1.983875 cm h = 5.23875 cm	80	18.85873
The moderator is full density water (0.9982 g/cm ³) surrounding three rings of double stacked slugs, each ring separated by a 277-4 canned spacer. (Slugs are inserted into the cylindrical geometry segment of the containment vessel using the hole option.) The contents (uranium and spacers) have an overall stack height of 22.83085 cm (8.98852 in.). No polyethylene was used in this model. Each ring is separated by a 3.5561 cm spacer and 0.0012 cm of moderating material. The bottom ring has a 0.0005 cm gap between it and the bottom of the containment vessel. The stack of slugs has 55.90865 cm of moderating material above. The modeled material masses are: 36.647 kg U (29.318 kg ²³⁵ U), 7.6434 kg H ₂ O, resulting in an h/x ratio of ~6.80. The loading arrangement of slugs is depicted in Fig. 6.9.1-4b for the Case cvcr5est11_2_2 .			

Table 6.9.1.1. Details of calculation models used to establish mass loading limits for surface-only modes of transportation identified in Table 6.2a

Case	Dimensions (cm)	Enrichment (wt. % ²³⁵ U)	Density (g/cm ³)
<i>Broken Metal for CSI=0.0</i>			
hciabmt12_4_1_5_3	r = 6.52620 cm h = 78.74000 cm	80	18.85873
The uranium "broken metal" content is homogenized with a moderator of water with a specific gravity of 1.0×10^{-4} over the interior volume of the containment vessel. No 277-4 canned spacers are used in this calculation. No polyethylene was used in this calculation. Since the contents are homogenized over the internal volume of the containment vessel, there is no moderating material between the content and the containment vessel walls. The modeled material masses are: 3.7085 kg U (2.9668 kg ²³⁵ U), 10.0007 kg H ₂ O, resulting in an h/x ratio of ~87.98.			
hciabmt12_5_1_4_3	r = 6.52620 cm h = 78.74000 cm	70	18.88264
The uranium "broken metal" content is homogenized with a moderator of water with a specific gravity of 1.0×10^{-4} over the interior volume of the containment vessel. No 277-4 canned spacers are used in this calculation. No polyethylene was used in this calculation. Since the contents are homogenized over the internal volume of the containment vessel, there is no moderating material between the content and the containment vessel walls. The modeled material masses are: 4.6415 kg U (3.2490 kg ²³⁵ U), 9.9516 kg H ₂ O, resulting in an h/x ratio of ~79.95.			
nciabmt11_6_1_3_3	r = 6.52620 cm h = 78.74000 cm	60	18.90661
The uranium "broken metal" content is homogenized with a moderator of water with a specific gravity of 1.0×10^{-4} over the interior volume of the containment vessel. No 277-4 canned spacers are used in this calculation. No polyethylene was used in this calculation. Since the contents are homogenized over the internal volume of the containment vessel, there is no moderating material between the content and the containment vessel walls. The modeled material masses are: 5.5768 kg U (3.3461 kg ²³⁵ U), 9.9025 kg H ₂ O, resulting in an h/x ratio of ~77.24.			
hciabmt12_3_2_8_3	r = 6.52620 cm h = 78.74000 cm	100	18.81109
The uranium "broken metal" content is homogenized with a moderator of water with a specific gravity of 1.0×10^{-4} over the interior volume of the containment vessel. The 277-4 canned spacers with a thickness of 3.5561 cm (1.4000 in.) are used and are modeled at 3.02984 cm and 9.61638 cm above the bottom of the containment vessel. No polyethylene was used in this calculation. Since the contents are homogenized over the internal volume of the containment vessel, there is no moderating material between the content and the containment vessel walls or the spacers. The modeled material masses are: 2.7743 kg ²³⁵ U, 9.4362 kg H ₂ O, resulting in an h/x ratio of ~88.78.			
hciabmt12_4_2_7_3	r = 6.52620 cm h = 78.74000 cm	95	18.82298
The uranium "broken metal" content is homogenized with a moderator of water with a specific gravity of 1.0×10^{-4} over the interior volume of the containment vessel. The 277-4 canned spacers with a thickness of 3.5561 cm (1.4000 in.) are used and are modeled at 3.02984 cm and 9.61638 cm above the bottom of the containment vessel. No polyethylene was used in this calculation. Since the contents are homogenized over the internal volume of the containment vessel, there is no moderating material between the content and the containment vessel walls or the spacers. The modeled material masses are: 3.7014 kg U (3.5164 kg ²³⁵ U), 9.3871 kg H ₂ O, resulting in an h/x ratio of ~69.68.			

Table 6.9.3.1-2. Summary for evaluation of HEU broken metal models (95 wt % ²³⁵U) in a flooded containment vessel, 1.4-in. canned spacers and full water reflection of containment vessel

Array type	U (g)	²³⁵ U (g)	H ₂ O (g)	h/x	<i>k</i> _{eff}	σ	<i>k</i> _{eff} + 2σ
discrete array of cubes ("sqa" cases)							
3 × 3 × <i>n</i>	35,164	33,406	7,719	6.03	0.8352	0.0012	0.84
6 × 6 × <i>n</i>	35,973	34,175	7,676	5.86	0.8559	0.0011	0.86
12 × 12 × <i>n</i>	35,988	34,188	7,765	5.86	0.8603	0.0012	0.86
cubes homogenized within footprint of lattice ("lha" cases)							
3 × 3 × <i>n</i>	35,164	33,406	7,719	6.03	0.8586	0.0011	0.86
6 × 6 × <i>n</i>	35,988	34,188	7,675	5.86	0.8650	0.0012	0.87
12 × 12 × <i>n</i>	35,988	34,188	7,675	5.86	0.8677	0.0010	0.87
cubes homogenized within containment vessel ("cha" cases)							
3 × 3 × <i>n</i>	35,164	33,406	7,719	6.03	0.9427	0.0013	0.95
6 × 6 × <i>n</i>	35,973	34,175	7,676	5.86	0.9495	0.0015	0.95
12 × 12 × <i>n</i>	35,988	34,188	7,675	5.86	0.9517	0.0016	0.95

The calculation results for the homogeneous mixture model of HEU metal and water within a rectangular lattice bound results for the explicit model. Also, the homogenization over the entire volume of the containment vessel is deemed overly conservative. For these reasons, the "lha" model is chosen to represent HEU broken metal inside the flooded containment vessel under full water reflection. For conservatism, the "cha" model is chosen to represent broken metal in single packages and the array of packages under NCT and HAC. Details regarding the "sqa", "lha", and "cha" calculation models are presented in Appendix 6.9.1.

HEU Oxide. Theoretical (crystalline) densities for HEU oxide are 10.96 g/cm³, 8.30 g/cm³, and 7.29 g/cm³ for UO₂, U₃O₈, and UO₃, respectively. While bulk densities of product oxides with enrichments ranging from 19 to 100 wt % ²³⁵U are typically on the order of 6.54 g/cm³, the bulk density of HEU oxides considered for shipment in the ES-3100 ranges from 2.0 to 6.54 g/cm³. Therefore, only less-than-theoretical mass loadings would actually be achieved. Skull oxides are a mixture of graphite and U₃O₈ with densities on the order of 2.44 g/cm³ for poured material and 2.78 g/cm³ for tapped material. The combined water saturation and crystallization of the HEU oxide are not expected in the HAC, given that UO₂ and UO₃ are non-hygroscopic while U₃O₈ is only mildly hygroscopic. Table 6.9.3.1-3 provides summary data for 292 samples of canned skull oxide.

Table 6.9.3.1-3. Summary data for 292 samples of skull oxide

Statistic	wt % U	wt % ²³⁵ U	μg C/g U	μg C/g ²³⁵ U	Net Wt (g)	U Wt (g)	²³⁵ U Wt (g)
Maximum	84.52	93.19	171,000	252,861	7,072	5,938	4,165
Minimum	12.93	20.28	13	17	442	312	221
Median	81.66	37.62	5,590	13,910	4,448	3,541	1,414
Mean	79.64	45.02	16,968	41,333	4,419	3,532	1,563
Std Dev	6.87	16.40	24,304	59,027	745	698	606

Values of wt % U, wt % ²³⁵U, μg C/g U, etc. for a given statistic (maximum, minimum, medium, or mean) do not occur simultaneously in a specific sample. Inspection of sample data reveals the following characteristics:

- (1) the fissile material content is <221 g ²³⁵U in samples with concentrations up to 252,861 μg C/g ²³⁵U,

- (2) the enrichment is 93.2 wt % ^{235}U for samples with concentrations in the range of 12,600 to 18,600 $\mu\text{g C/gU}$,
- (3) the enrichment ranges from 60 to 70.2 wt % ^{235}U for samples with concentrations in the range of 3,231 to 87,720 $\mu\text{g C/gU}$, and
- (4) the enrichment ranges from 37 to 38 wt % ^{235}U for samples with concentrations in the range of 400 to 233,366 $\mu\text{g C/gU}$.

Eight skull oxide compositions representative of 292 samples of canned skull oxide were selected for establishing the bounding content calculation models. The skull oxide content is assumed to be U_3O_8 plus graphite, polyethylene, and unidentified material. Two additional compositions were derived for addressing skull oxides with an enrichment of 93.2 wt % ^{235}U where unidentified material is treated as ^{235}U and the carbon content is either maximized or minimized. Treatment of the unidentified material as fissile material in the criticality analysis assures that its presence in skull oxide does not increase reactivity beyond what is considered in the bounding analysis.

The composition of the skull oxide content is given in terms of the following parameters: the grams skull oxide content in a content can (**gramskul**), the content bulk density (**densoc**), the wt % uranium in skull oxide content (**wtpuskul**), the wt % ^{235}U in uranium (**wtpu25u**), and the grams of graphite in the content can (**gramg**). Values for the content specification parameters are provided in Table 6.9.3.1-3b.

Table 6.9.3.1-3b. Content specification parameters for skull oxide content

Content	gramskul (g)	densoc (g/cm ³)	wtpuskul (wt %)	wtpu25u (wt %)	gramg (g)
sk_01	3863	1.899	58.92	69.78	139
sk_02	4978	2.447	66.15	69.42	168
sk_03	4607	1.981	72.77	69.88	124
sk_04	5082	2.186	82.77	70.07	20
sk_05	7072	3.042	83.97	69.91	9
sk_06	5037	2.476	72.53	37.61	307
sk_07	4385	2.156	75.15	37.55	203
sk_08	4550	2.237	72.57	37.73	87
sk_09	7100	3.054	78.95	93.20	307
sk_10	7100	3.054	82.61	93.20	1.0E-05

The information in Table 6.9.3.1-3c is derived from the content specification parameters of Table 6.9.3.1-3b on the assumption that 513 g of polyethylene is present in the skull oxide content in three content locations inside the containment vessel.

The amount of skull oxide content (Column 2, Table 6.9.3.1-3c) is $\text{gsoc} = 3.0 \times \text{gramskul}$.

The amount of uranium in the skull oxide content (Column 6, Table 6.9.3.1-3c) is $\text{gusoc} = \text{gsoc} \times \text{wtpuskul} / 100.0$.

The amount of ^{235}U (Column 7, Table 6.9.3.1-3c) is $\text{gr235} = \text{gusoc} \times \text{wtpu25u} / 100.0$.

The amount of graphite in the skull oxide content (Column 8, Table 6.9.3.1-3c) is $\text{ggsoc} = 3.0 \times \text{gramg}$.

The micrograms graphite per gram uranium in skull oxide content (Column 9, Table 6.9.3.1-3c) is $\text{mggraphgu} = \text{ggsoc} \times 1.0\text{e}6 / \text{gusoc}$.

The amount of U_3O_8 in the skull oxide content (**guox**) [Column 3, Table 6.9.3.1-3c] is $\text{guox} = \text{gsoc} / \text{wtpuox}$,

Appendix 6.9.6

ABRIDGED SUMMARY TABLES OF CRITICALITY CALCULATION RESULTS

This appendix contains the summary tables for calculation results identified in Sects. 6.4, 6.5, 6.6, and 6.7 of this document. The CV calculation model is a modification of the water-reflected, single-unit package calculation model where the packaging regions external to the containment vessel are replaced with full density water. The index is as follows:

CYLINDER CONTENT

Table 6.9.6-1 Results for the 3.24-in.-diam cylinder HEU content in CV calculation model.

Table 6.9.6-2 Results for the 3.24-in.-diam cylinder HEU content in bare and water reflected package calculation models.

Table 6.9.6-3 Results for the 3.24-in.-diam cylinder HEU content in package calculation models.

Table 6.9.6-3b Results for spacing of 3.24 in.-diameter cylinder HEU metal content in CV calculation model.

Table 6.9.6-3c Results for spacing of 3.24 in.-diameter cylinder HEU metal content in packaging calculation model.

SQUARE BAR CONTENT

Table 6.9.6-4 Results for the 2.29-in square bar HEU content in CV calculation model.

Table 6.9.6-5 Results for the 2.29-in square bar HEU content in packaging calculation model.

CYLINDER CONTENT

Table 6.9.6-6 Results for the 4.25-in.-diam cylinder HEU content in CV calculation model.

Table 6.9.6-7 Results for the 4.25-in.-diam cylinder HEU content in packaging calculation models.

SLUGS CONTENT

Table 6.9.6-8 Results for 1.5-in.-diam \times 2.0-in.-tall slug HEU metal content in CV calculation model.

Table 6.9.6-9 Results for the 1.5-in.-diam \times 2.0-in.-tall slug HEU metal content in packaging calculation model.

BROKEN METAL CONTENT

Table 6.9.6-10 Results for HEU broken metal content in CV calculation model.

Table 6.9.6-11 Results for HEU broken metal content in packaging calculation model.

Table 6.9.6-11b Comparison of NCT results for HEU broken metal content in ES-3100 NCT packaging calculation models

Table 6.9.6-11c Comparison of HAC results for HEU broken metal content in ES-3100 HAC packaging calculation models

HEU PRODUCT OXIDE CONTENT

- Table 6.9.6-12 Results for HEU oxide content in CV calculation model.
- Table 6.9.6-13 Results for HEU product oxide content at 6.54 g/cm³ in single-unit packaging calculation model.
- Table 6.9.6-13a Results for HEU oxide content in single-unit packaging calculation model.
- Table 6.9.6-13b Results for HEU oxide content in array packaging calculation model.

UNX CRYSTAL CONTENT

- Table 6.9.6-14 Results for UNX crystal content in CV calculation model.
- Table 6.9.6-15 Results for UNX crystal content in packaging calculation model.
- Table 6.9.6-16 Results for leakage of UNX crystal content out of containment vessel.

HEU SKULL OXIDE CONTENT

- Table 6.9.6-17 Results for skull oxide (SO) content in CV calculation model.
- Table 6.9.6-18a NCT results for SO content in packaging calculation model.
- Table 6.9.6-18b HAC results for SO content in packaging calculation model.

UNIRRADIATED TRIGA REACTOR FUEL ELEMENT CONTENT

- Table 6.9.6-19a Results for UZrH_x content in CV calculation model.
- Table 6.9.6-19b Results for UZrH_x content spacing in CV calculation model.
- Table 6.9.6-19c Results for UZrH_x content uranium weight fraction in CV calculation model.
- Table 6.9.6-20a Results for UZrH_x content at 19.7 wt % ²³⁵U in packaging calculation model.
- Table 6.9.6-20b Results for UZrH_x content at 70.1 wt % ²³⁵U in packaging calculation model.
- Table 6.9.6-20c Results for 1.31 in. Smaller diameter UZrH_x at 70.1 wt % ²³⁵U content in packaging calculation model.
- Table 6.9.6-20d Results for 1.31 in. smaller diameter UZrH_x at 19.7 wt % ²³⁵U content in packaging calculation model.

AIR TRANSPORT CONTENT

- Table 6.9.6-21 Results for solid HEU metal content for air transportation.
- Table 6.9.6-22a Results for TRIGA (UZrH_x) fuel element content at 19.7 wt % ²³⁵U for air transportation.
- Table 6.9.6-22b Results for TRIGA (UZrH_x) fuel element content at 70.1 wt % ²³⁵U for air transportation.
- Table 6.9.6-22c Results for research reactor fuel (U₃O₈-Al) content for air transportation.
- Table 6.9.6-22d Results for research reactor fuel (UO₂-Mg with clad Al) content for air transportation.
- Table 6.9.6-23 Results for HEU broken metal content for air transport.

Table 6.9.6-12. Results for HEU oxide content in CV calculation model

case name (cvcprpdoxt11)	Ox (g)	²³⁵ U (g)	Ox density (g/cm ³)	Ox volume (cm ³)	Sat. H ₂ O (g)	CV H ₂ O (g)	h/x	mocfr	k _{eff}	σ	k _{eff} +2σ
UO₂ content, 500 g polyethylene, flooded containment vessel, reflected											
_1_3_24_15	24000	21125	4.00	6000	3803	3665	10.02	1.0e+00	0.91157	0.00138	0.91434
_1_4_24_15	24000	21125	5.00	4800	2606	4863	10.02	1.0e+00	0.90264	0.00139	0.90541
_1_5_24_15	24000	21125	6.54	5000	1477	5991	10.02	1.0e+00	0.89152	0.00115	0.89382
_1_2_20_15	20000	17604	3.00	6667	4833	3000	12.57	1.0e+00	0.90943	0.00117	0.91177
_1_3_20_15	20000	17604	4.00	5000	3170	4663	12.57	1.0e+00	0.89797	0.00129	0.90055
_1_4_20_15	20000	17604	5.00	4000	2171	5662	12.57	1.0e+00	0.89035	0.00121	0.89278
_1_5_20_15	20000	17604	6.54	3058	1231	6602	12.57	1.0e+00	0.87565	0.00112	0.87789
_1_2_15_15	15000	13203	3.00	5000	3625	4664	17.66	1.0e+00	0.89891	0.00138	0.90166
_1_3_15_15	15000	13203	4.00	3750	2377	5911	17.66	1.0e+00	0.87963	0.00116	0.88195
_1_4_15_15	15000	13203	5.00	3000	1629	6660	17.66	1.0e+00	0.86309	0.00134	0.86578
_1_5_15_15	15000	13203	6.54	2294	923	7365	17.66	1.0e+00	0.84270	0.00121	0.84513
14,000 g UO₂ content, 500 g polyethylene, flooded containment vessel, reflected											
_1_1_14_15	14000	12323	2.00	7000	5712	2667	19.11	1.0e+00	0.90801	0.00154	0.91110
_1_2_14_15	14000	12323	3.00	4667	3383	4996	19.11	1.0e+00	0.89261	0.00124	0.89510
_1_3_14_15	14000	12323	4.00	3500	2219	6161	19.11	1.0e+00	0.87604	0.00119	0.87842
_1_4_14_15	14000	12323	5.00	2800	1520	6860	19.11	1.0e+00	0.85585	0.00139	0.85863
_1_5_14_15	14000	12323	6.54	2141	862	7518	19.11	1.0e+00	0.83530	0.00112	0.83755
14,000 g U₃O₈ content, 500 g polyethylene, flooded containment vessel, reflected											
_2_1_14_15	14000	11850	2.00	7000	5304	2667	18.97	1.0e+00	0.88331	0.00144	0.88620
_2_2_14_15	14000	11850	3.00	4667	2975	4996	18.97	1.0e+00	0.85075	0.00129	0.85333
_2_3_14_15	14000	11850	4.00	3500	1810	6161	18.97	1.0e+00	0.82386	0.00123	0.82632
_2_4_14_15	14000	11850	5.00	2800	1111	6860	18.97	1.0e+00	0.79922	0.00143	0.80209
_2_5_14_15	14000	11850	6.54	2141	453	7518	18.97	1.0e+00	0.76510	0.00114	0.76738

Table 6.9.6-12. Results for HEU oxide content in CV calculation model

case name (cvcprdoxt11)	Ox (g)	²³⁵ U (g)	Ox density (g/cm ³)	Ox volume (cm ³)	Sat. H ₂ O (g)	CV H ₂ O (g)	h/x	mocfr	k _{eff}	σ	k _{eff} +2σ
14,000 g UO₃ content, 500 g polyethylene, flooded containment vessel, reflected											
3_1_14_15	14000	11627	2.00	7000	5071	2667	18.81	1.0e+00	0.86835	0.00122	0.87079
3_2_14_15	14000	11627	3.00	4667	2741	4996	18.81	1.0e+00	0.83069	0.00119	0.83307
3_3_14_15	14000	11627	4.00	3500	1577	6161	18.81	1.0e+00	0.79457	0.00132	0.79720
3_4_14_15	14000	11627	5.00	2800	878	6860	18.81	1.0e+00	0.76399	0.00140	0.76679
3_5_14_15	14000	11627	6.54	2141	220	7518	18.81	1.0e+00	0.72235	0.00127	0.72490
14,000 g UO₂ content, 500 g polyethylene, dry containment vessel, reflected											
1_1_14_1	14000	12323	2.00	7000	5712	0	13.46	1.0e-20	0.90869	0.00156	0.91180
1_2_14_1	14000	12323	3.00	4667	3383	0	8.53	1.0e-20	0.88628	0.00144	0.88916
1_3_14_1	14000	12323	4.00	3500	2219	0	6.06	1.0e-20	0.86750	0.00131	0.87012
1_4_14_1	14000	12323	5.00	2800	1520	0	4.58	1.0e-20	0.84555	0.00151	0.84857
1_5_14_1	14000	12323	6.54	2141	862	0	3.19	1.0e-20	0.82157	0.00109	0.82375
UO₂ content, 2.0 g/cm³ oxide density, 500 g polyethylene, flooded containment vessel, reflected											
1_1_14_15	14000	12323	2.00	7000	5712	2667	19.11	1.0e+00	0.90801	0.00154	0.91110
1_1_13_15	13000	11443	2.00	6500	5304	3166	20.79	1.0e+00	0.91011	0.00123	0.91258
1_1_12_15	12000	10562	2.00	6000	4896	3665	22.74	1.0e+00	0.90176	0.00141	0.90457
1_1_11_15	11000	9682	2.00	5500	4488	4164	25.06	1.0e+00	0.89737	0.00154	0.90044
1_1_10_15	10000	8802	2.00	5000	4080	4663	27.83	1.0e+00	0.89620	0.00130	0.89880
1_1_9_15	9000	7922	2.00	4500	3672	5163	31.23	1.0e+00	0.88551	0.00161	0.88872
1_1_8_15	8000	7042	2.00	4000	3264	5662	35.47	1.0e+00	0.87598	0.00157	0.87912
1_1_7_15	7000	6162	2.00	3500	2856	6161	40.92	1.0e+00	0.86765	0.00148	0.87061
1_1_6_15	6000	5281	2.00	3000	2448	6660	48.19	1.0e+00	0.85412	0.00120	0.85652
1_1_5_15	5000	4401	2.00	2500	2040	7159	58.37	1.0e+00	0.83022	0.00138	0.83298
1_1_4_15	4000	3521	2.00	2000	1632	7658	73.63	1.0e+00	0.80856	0.00156	0.81168
1_1_3_15	3000	2641	2.00	1500	1224	8157	99.08	1.0e+00	0.77245	0.00147	0.77539
1_1_2_15	2000	1761	2.00	1000	816	8656	149.96	1.0e+00	0.72062	0.00132	0.72326
1_1_1_15	1000	880	2.00	500	408	9155	302.58	1.0e+00	0.63401	0.00126	0.63653

Table 6.9.6-13. Results for HEU product oxide content at 6.54 g/cm³ in single-unit packaging calculation model

case name	Ox (g)	²³⁵ U (g)	Sat. H ₂ O (g)	CV H ₂ O (g)	h/x	moifr	k _{eff}	σ	k _{eff} +2σ	case name	k _{eff}	σ	k _{eff} +2σ
UO₂ content and 500 g polyethylene in flooded containment vessel, single package reflected													
NCT										HAC			
ncsrpox11_1_24_1	24000	21125	1477	5991	10.02	1.0e-20	0.72148	0.00120	0.72388				
ncsrpox11_1_24_2	24000	21125	1477	5991	10.02	1.0e-05	0.71942	0.00107	0.72156				
ncsrpox11_1_24_3	24000	21125	1477	5991	10.02	0.0e+00	0.71790	0.00122	0.72035				
ncsrpox11_1_24_4	24000	21125	1477	5991	10.02	1.0e-03	0.72072	0.00154	0.72380				
ncsrpox11_1_24_5	24000	21125	1477	5991	10.02	1.0e-02	0.71999	0.00123	0.72244				
ncsrpox11_1_24_6	24000	21125	1477	5991	10.02	1.0e-01	0.72828	0.00103	0.73035				
ncsrpox11_1_24_8	24000	21125	1477	5991	10.02	3.0e-01	0.74362	0.00123	0.74607				
ncsrpox11_1_24_15	24000	21125	1477	5991	10.02	1.0e+00	0.80222	0.00108	0.80438				

Table 6.9.6-13a. Results for HEU oxide content in single-unit packaging calculation model

case name (ncsrpdoxt11)	Ox (g)	²³⁵ U (g)	Ox den. (g/cm ³)	Ox vol. (cm ³)	Sat. H ₂ O (g)	CV H ₂ O (g)	h/x	k _{eff}	σ	k _{eff} +2σ	case name (hcsrpdopt12)	k _{eff}	σ	k _{eff} +2σ
UO₂ content and 500 g polyethylene in flooded containment vessel, flooded package														
NCT											HAC			
_1_3_24	24000	21125	4.00	6000	3803	3665	10.02	0.81371	0.00144	0.81659	_1_3_24	0.81599	0.00133	0.81865
_1_4_24	24000	21125	5.00	4800	2606	4863	10.02	0.80666	0.00111	0.80887	_1_4_24	0.81112	0.00119	0.81350
_1_5_24	24000	21125	6.54	3670	1477	5991	10.02	0.80222	0.00108	0.80438	_1_5_24	0.80624	0.00114	0.80852
_1_2_20	20000	17604	3.00	6667	4833	3000	12.57	0.81352	0.00155	0.81662	_1_2_20	0.81200	0.00136	0.81472
_1_3_20	20000	17604	4.00	5000	3170	4663	12.57	0.80451	0.00124	0.80698	_1_3_20	0.80524	0.00118	0.80760
_1_4_20	20000	17604	5.00	4000	2171	5662	12.57	0.79655	0.00129	0.79914	_1_4_20	0.79813	0.00137	0.80087
_1_5_20	20000	17604	6.54	3058	1231	6602	12.57	0.78510	0.00133	0.78775	_1_5_20	0.78801	0.00121	0.79043
_1_2_15	15000	13203	3.00	5000	3625	4664	17.66	0.79666	0.00133	0.79933	_1_2_15	0.79891	0.00149	0.80189
_1_3_15	15000	13203	4.00	3750	2377	5911	17.66	0.78374	0.00123	0.78619	_1_3_15	0.78801	0.00130	0.79061

Table 6.9.6-13a. Results for HEU oxide content in single-unit packaging calculation model

case name (ncsrpdoxt11)	Ox (g)	²³⁵ U (g)	Ox den. (g/cm ³)	Ox vol. (cm ³)	Sat. H ₂ O (g)	CV H ₂ O (g)	h/x	k _{eff}	σ	k _{eff} +2σ	case name (hcsrpdoxt12)	k _{eff}	σ	k _{eff} +2σ
_1_4_15	15000	13203	5.00	3000	1629	6660	17.66	0.77585	0.00104	0.77794	_1_4_15	0.77767	0.00131	0.78028
_1_5_15	15000	13203	6.54	2294	923	7365	17.66	0.75988	0.00120	0.76228	_1_5_15	0.76047	0.00122	0.76291
UO₂ content and 500 g polyethylene in flooded containment vessel, flooded package														
NCT											HAC			
_1_1_14	14000	12323	2.00	7000	5712	2667	19.11	0.81144	0.00130	0.81403	_1_1_14	0.80983	0.00147	0.81276
_1_2_14	14000	12323	3.00	4667	3383	4996	19.11	0.79632	0.00134	0.79900	_1_2_14	0.79412	0.00155	0.79722
_1_3_14	14000	12323	4.00	3500	2219	6161	19.11	0.78024	0.00138	0.78300	_1_3_14	0.78251	0.00141	0.78533
_1_4_14	14000	12323	5.00	2800	1520	6860	19.11	0.76867	0.00119	0.77106	_1_4_14	0.77186	0.00130	0.77446
_1_5_14	14000	12323	6.54	2141	862	7518	19.11	0.75106	0.00143	0.75393	_1_5_14	0.75712	0.00132	0.75975
UO₃ content and 500 g polyethylene in flooded containment vessel, flooded package														
_2_1_14	14000	11850	2.00	7000	5304	2667	18.97	0.77449	0.00162	0.77772	_2_1_14	0.77571	0.00138	0.77847
_2_2_14	14000	11850	3.00	4667	2975	4996	18.97	0.75132	0.00141	0.75415	_2_2_14	0.74985	0.00135	0.75256
_2_3_14	14000	11850	4.00	3500	1810	6161	18.97	0.72213	0.00119	0.72452	_2_3_14	0.72485	0.00112	0.72708
_2_4_14	14000	11850	5.00	2800	1111	6860	18.97	0.70025	0.00132	0.70289	_2_4_14	0.70229	0.00135	0.70498
_2_5_14	14000	11850	6.54	2141	453	7518	18.97	0.66897	0.00140	0.67177	_2_5_14	0.67431	0.00107	0.67645
U₃O₈ content and 500 g polyethylene in flooded containment vessel, flooded package														
_3_1_14	14000	11627	2.00	7000	5071	2667	18.81	0.75704	0.00138	0.75980	_3_1_14	0.75676	0.00139	0.75954
_3_2_14	14000	11627	3.00	4667	2741	4996	18.81	0.72097	0.00124	0.72345	_3_2_14	0.72300	0.00121	0.72542
_3_3_14	14000	11627	4.00	3500	1577	6161	18.81	0.69035	0.00114	0.69263	_3_3_14	0.69274	0.00112	0.69498
_3_4_14	14000	11627	5.00	2800	878	6860	18.81	0.66080	0.00123	0.66326	_3_4_14	0.66443	0.00115	0.66674
_3_5_14	14000	11627	6.54	2141	220	7518	18.81	0.62168	0.00129	0.62427	_3_5_14	0.62544	0.00118	0.62780

Table 6.9.6-13b. Results for HEU oxide content in array packaging calculation model

case name (nciapdoxt11)	Ox (g)	²³⁵ U (g)	Ox den. (g/cm ³)	Ox vol. (cm ³)	Sat. H ₂ O (g)	CV H ₂ O (g)	h/x	k _{eff}	σ	k _{eff} +2σ	case name (nciapdoxt12)	k _{eff}	σ	k _{eff} +2σ
UO ₂ content and 500 g polyethylene in flooded containment vessel, array packaging model for CSI=0.0														
NCT											HAC			
1_3_24_3	24000	21125	4.00	6000	3803	3665	10.02	0.96758	0.00121	0.97000	1_3_24_3	0.96822	0.00124	0.97070
1_4_24_3	24000	21125	5.00	4800	2606	4863	10.02	0.94340	0.00119	0.94578	1_4_24_3	0.94131	0.00115	0.94360
1_5_24_3	24000	21125	6.54	3670	1477	5991	10.02	0.91495	0.00134	0.91764	1_5_24_3	0.91666	0.00106	0.91878
1_2_20_3	20000	17604	3.00	6667	4833	3000	12.57	0.97118	0.00122	0.97363	1_2_20_3	0.97255	0.00139	0.97532
1_3_20_3	20000	17604	4.00	5000	3170	4663	12.57	0.93543	0.00122	0.93786	1_3_20_3	0.93616	0.00141	0.93897
1_4_20_3	20000	17604	5.00	4000	2171	5662	12.57	0.91167	0.00117	0.91401	1_4_20_3	0.91202	0.00126	0.91453
1_5_20_3	20000	17604	6.54	3058	1231	6602	12.57	0.88413	0.00124	0.88661	1_5_20_3	0.88426	0.00137	0.88700
1_2_15_3	15000	13203	3.00	5000	3625	4664	17.66	0.92181	0.00128	0.92438	1_2_15_3	0.92129	0.00139	0.92407
1_3_15_3	15000	13203	4.00	3750	2377	5911	17.66	0.88533	0.00117	0.88767	1_3_15_3	0.88414	0.00125	0.88663
1_4_15_3	15000	13203	5.00	3000	1628	6660	17.66	0.86168	0.00116	0.86400	1_4_15_3	0.86039	0.00117	0.86273
1_5_15_3	15000	13203	6.54	2294	923	7365	17.66	0.83434	0.00122	0.83678	1_5_15_3	0.83140	0.00111	0.83363
1_1_12_3	12000	10562	2.00	6000	4896	3665	22.74	0.93409	0.00140	0.93688	1_1_12_3	0.93732	0.00137	0.94006
1_2_12_3	12000	10562	3.00	4000	2900	5662	22.74	0.88391	0.00131	0.88652	1_2_12_3	0.88387	0.00121	0.88630
1_3_12_3	12000	10562	4.00	3000	1902	6660	22.74	0.85157	0.00111	0.85379	1_3_12_3	0.84658	0.00133	0.84925
1_4_12_3	12000	10562	5.00	2400	1303	7259	22.74	0.82574	0.00128	0.82831	1_4_12_3	0.82349	0.00119	0.82587
1_5_12_3	12000	10562	6.54	1835	739	7823	22.74	0.79328	0.00110	0.79548	1_5_12_3	0.79233	0.00121	0.79475
1_1_11_3	11000	9682	2.00	5500	4488	4164	25.06	0.91822	0.00129	0.92079	1_1_11_3	0.92203	0.00134	0.92471
1_2_11_3	11000	9682	3.00	3667	2658	5994	25.06	0.86689	0.00129	0.86946	1_2_11_3	0.87093	0.00135	0.87364
1_3_11_3	11000	9682	4.00	2750	1743	6909	25.06	0.83492	0.00133	0.83757	1_3_11_3	0.83515	0.00124	0.83763
1_4_11_3	11000	9682	5.00	2200	1194	7458	25.06	0.80930	0.00149	0.81227	1_4_11_3	0.80948	0.00129	0.81205
1_5_11_3	11000	9682	6.54	1682	677	7976	25.06	0.77906	0.00100	0.78106	1_5_11_3	0.77935	0.00118	0.78171
1_1_10_3	10000	8802	2.00	5000	4080	4663	27.83	0.90471	0.00131	0.90733	1_1_10_3	0.90600	0.00128	0.90856
1_1_9_3	9000	7922	2.00	4500	3672	5163	31.23	0.88936	0.00137	0.89210	1_1_9_3	0.88714	0.00123	0.88960
1_1_8_3	8000	7042	2.00	4000	3264	5662	35.47	0.86854	0.00144	0.87141	1_1_8_3	0.86980	0.00145	0.87270
1_1_7_3	7000	6162	2.00	3500	2856	6161	40.92	0.84876	0.00125	0.85126	1_1_7_3	0.84926	0.00133	0.85192

Table 6.9.6-13b. Results for HEU oxide content in array packaging calculation model

case name (nciapdopt11)	Ox (g)	²³⁵ U (g)	Ox den. (g/cm ³)	Ox vol. (cm ³)	Sat. H ₂ O (g)	CV H ₂ O (g)	h/x	k _{eff}	σ	k _{eff} +2σ	case name (nciapdopt12)	k _{eff}	σ	k _{eff} +2σ
_1_1_6_3	6000	5281	2.00	3000	2448	6660	48.19	0.82546	0.00127	0.82800	_1_1_6_3	0.82275	0.00135	0.82544
UO₂, UO₃, or U₃O₈ content and 500 g polyethylene in flooded containment vessel, array packaging model for CSI=0.0														
_1_1_7_3	7000	6162	2.00	3500	2856	6161	40.92	0.84876	0.00125	0.85126	_1_1_7_3	0.84926	0.00133	0.85192
_2_1_7_3	7000	5925	2.00	3500	2652	6161	41.65	0.81721	0.00130	0.81980	_2_1_7_3	0.81943	0.00125	0.82194
_3_1_7_3	7000	5813	2.00	3500	2535	6161	41.93	0.80044	0.00129	0.80302	_3_1_7_3	0.80086	0.00134	0.80355

Table 6.9.6-14. Results for UNX crystal content in CV calculation model

case name	unh (g)	²³⁵ U (g)	unh H ₂ O (g)	CV H ₂ O (g)	h/x	gU/l	mocfr	k _{eff}	σ	k _{eff} +2σ				
UNH crystal content, 0 g polyethylene, flooded containment vessel, reflected														
cvcrunhct11_24_1	24000	11303	5197	1620	15.74	1106	1.0e+00	0.82007	0.00128	0.82262				
cvcrunhct11_23_1	23000	10832	4980	1978	16.77	1060	1.0e+00	0.82120	0.00129	0.82378				
cvcrunhct11_22_1	22000	10361	4764	2335	17.88	1014	1.0e+00	0.82675	0.00122	0.82919				
cvcrunhct11_21_1	21000	9890	4547	2693	19.11	968	1.0e+00	0.82938	0.00118	0.83174				
cvcrunhct11_20_1	20000	9419	4331	3050	20.45	922	1.0e+00	0.83221	0.00129	0.83480				
cvcrunhct11_19_1	19000	8948	4114	3407	21.94	876	1.0e+00	0.83423	0.00152	0.83728				
cvcrunhct11_18_1	18000	8477	3898	3765	23.59	830	1.0e+00	0.83622	0.00128	0.83878				
cvcrunhct11_17_1	17000	8006	3681	4122	25.44	784	1.0e+00	0.84032	0.00167	0.84365				
cvcrunhct11_16_1	16000	7536	3464	4479	27.51	738	1.0e+00	0.84509	0.00151	0.84811				
cvcrunhct11_15_1	15000	7064	3248	4837	29.87	692	1.0e+00	0.84402	0.00133	0.84667				
cvcrunhct11_14_1	14000	6594	3031	5194	32.56	645	1.0e+00	0.84915	0.00130	0.85175				
cvcrunhct11_13_1	13000	6123	2815	5551	35.67	599	1.0e+00	0.84986	0.00127	0.85241				
cvcrunhct11_12_1	12000	5652	2598	5909	39.29	553	1.0e+00	0.85138	0.00159	0.85456				
cvcrunhct11_11_1	11000	5181	2382	6266	43.57	507	1.0e+00	0.85137	0.00136	0.85408				
cvcrunhct11_10_1	10000	4710	2165	6623	48.71	461	1.0e+00	0.85062	0.00149	0.85359				
cvcrunhct11_9_1	9000	4239	1949	6981	54.99	415	1.0e+00	0.85423	0.00147	0.85718				

7.1.3 Preparation for Transport

7.1.3.1 Package Handling

Criticality Safety Index (CSI) values for the ES-3100 package with various payloads can be found in Table 1.3.

The ES-3100 is handled using industry-standard drum-handling equipment. Operating procedures shall include requirements to limit clamping pressures on forklift drum-handling equipment to prevent damage to the ES-3100 drum body (see Sect. 1.2.1.1 for limits on forklift gripping forces).

7.1.3.2 Decontamination

The package may be placed onto areas that are covered by disposable covering, such as plastic or paper, to reduce the nonfixed surface contamination of physical structures.

The package must be shipped in an enclosed conveyance. Generally, the exterior surfaces of the package will remain relatively clean. However, each user shall prepare procedures to clean dirty packages. These procedures shall, at a minimum, consider the following:

1. The drum is austenitic stainless steel.
2. The drum nut is silicon bronze.
3. The drum vent holes are covered with plastic push-in plugs.
4. The labels and markings on the drum must remain legible.
5. The cleaning solution must be checked for contamination.

7.1.3.3 Requirements Prior to Shipment

The shipper shall ensure that the quality control requirements of 49 CFR 173.475 and the routine determination requirements of 10 CFR 71.87 have been satisfied prior to each shipment. Detailed operating procedures [10 CFR 71.87(f)], shall provide evidence that these requirements are met and ensure that:

1. the package is proper for the content shipped and verified with the appropriate records by the user prior to content loading [10 CFR 71.87(a)];
2. when shipping uranium oxides or UNX crystals, the shipper shall provide the receiver with the date and time the containment vessel was sealed. The shipper must verify that the shipment can be completed within the time period allotted for the type of shipment (5 months or 1 year for UNX crystals as noted in Table 1.3a or 1 year for uranium oxides);
3. the package is in unimpaired physical condition [10 CFR 71.87(b)];
4. the closure devices of the package are properly installed, secured, and free of defects [10 CFR 71.87(c)];
5. the containment vessel has been loaded properly and preparation for shipment has been followed, witnessed, and checked;

6. the internal pressure of the containment system does not exceed the design pressure during transportation [10 CFR 71.85(b)] as demonstrated by analysis (Appendix 2.10.1) and that there are no pressure-relief devices [10 CFR 71.87(e)] in the package;
7. the external radiation levels for all transport conditions are within the allowable limits as measured for Normal Conditions of Transport (NCT) [10 CFR 71.87(j)];
8. the nonfixed external contamination levels are within the allowable limits as demonstrated by surface wipes prior to content insertion, containment vessel loading, and package closure [10 CFR 71.87(I)];
9. the contents are adequately sealed and have adequate space for expansion [10 CFR 71.87(d)];
10. all records for shipment are prepared and maintained; and
11. all lifting attachment features are either inoperative during transport [10 CFR 71.87(h)] or meet the requirements of 10 CFR 71.45(a).

7.1.3.4 Leak Testing

Leak tests shall be conducted following the content loading and the containment vessel closure. The annulus between the O-rings shall be leak tested to an acceptable leak rate of 1×10^{-4} ref-cm³/s air (or equivalent) or lower in accordance with ANSI N14.5-1997, Subclause 7.6.

7.1.3.5 Surveying

The radiation (gamma, neutron) emanating from the contents of the package shall be measured before the package is released for transport [10 CFR 71.47 and 71.87(j)]. The package radiation dose rate at the surface is measured to ensure that the content does not exceed the expected or allowable dose rates. The package radiation dose rate at 1 m from the surface is measured to establish the TI for the package. The package exterior surface contamination level limits are found in 10 CFR 71.87(i) and 49 CFR 173.443. The regulations present both fixed and nonfixed surface contamination level limits for the various radionuclides. In addition to these limits, the user may have more stringent surface contamination levels that shall also be followed.

A final visual survey of the package and loading paperwork shall be conducted to ensure that the package was assembled correctly and that it is ready for final shipment preparation. This survey may include a thorough review of the loading checklists by someone other than those who filled out the list to verify the loading operations. The area immediately surrounding the assembly operations should be surveyed, and all spare or extra parts should be identified. A final package survey may include weighing the package, hand-testing the closure nuts on the drum lid, and flexing the TIDs. The loading checklist should include a place for this final quality check to be properly recorded—including a signature and date—as being successfully completed.

7.1.3.6 Marking

The user shall ensure detailed marking procedures are consistent with 10 CFR 71.85 and the applicable subsections of 49 CFR 172, Subpart D. Each shipper shall ensure that each package containing radioactive material is marked in the manner required.

Two electrochemically etched data plates are affixed to the exterior of the drum body in the locations, and with the methods, indicated on Drawing M2E801580A031 (Appendix 1.4.8).

The packaging components (drum assembly, containment vessel body, lid, and closure nut) are also marked with their serial numbers. The numbers are used to control these parts and to accumulate their respective histories.

7.1.3.7 Labeling

The user shall prepare labeling procedures that are consistent with the applicable subsections of 49 CFR 172, Subpart E. The procedures should include the following steps, to ensure that:

1. the proper label is affixed to the package and the TI is determined at the time of loading;
2. the correct label (White—I, Yellow—II, or Yellow-III) is determined using the table from 49 CFR 172.403(c);
3. the appropriate label is affixed to two places on opposite sides of the drum;
4. the content name, nuclides and activity/mass (49 CFR 173.435), and the TI are entered in the blank spaces on the radioactive label; and
5. the information is entered legibly using a durable, weather-resistant means of marking.

Additionally, two Fissile labels are required per 49 CFR 172.402(d)(2). These labels must be affixed two places on opposite sides of the drum adjacent to the radioactive labels. The CSI must be legibly entered on the Fissile label using a durable, weather-resistant means of marking.

7.1.3.8 Securing to Vehicle

The package shall be secured against movement within the vehicle in which it is being transported under conditions normally incident to transportation [49 CFR 177.834 and 177.842(d)]. The loading procedures shall include the following measures, at a minimum, to ensure that:

1. only an approved conveyance is used,
2. all reasonable precautions are taken to prevent motion of the vehicle during loading,
3. no tampering with packages occurs during transit,
4. no vehicle is loaded or unloaded unless a qualified person is in attendance at all times, and
5. no radioactive material package is loaded onto a vehicle also carrying Div. 1.1 or 1.2 explosives (49 CFR 177.848).

7.2 PACKAGE UNLOADING

7.2.1 Receipt of Package from Carrier

Prior to shipment, the user shall verify that the receiver has agreed to accept the special nuclear material. The user (shipper) shall ensure that appropriate documentation is submitted to the receiver to ensure that the physical characteristics and hazards of the material are conveyed to the receiver.

The user shipping the package shall provide any special instructions to the receiver to safely open the package (10 CFR 71.89), including special tools and precautions for handling or unloading. These instructions shall include special actions in the event that TIDs are not intact, or if surface contamination or radiation surveys are too high.

The receiver shall check the seal time and date before opening the container. The receiver shall open the CV prior to the seal time expiring or take special precautions when handling and opening the container. Special precautions are associated with the potential buildup of hydrogen in the CV to greater than 5 mol %. Typical precautions may include, but are not limited to, elimination of ignition sources, gradually opening the CV in a well-ventilated area, or opening the CV in an inert glove box.

The receiver shall accept the radioactive material by surveying the conveyance and package surface for contamination and external radiation levels. The receiver's procedures shall clearly indicate that the contamination and radiation surveys and inspections be conducted upon receipt of the package. The receiver shall, at a minimum, include the following in their procedures (in compliance with 10 CFR 71.111):

1. receive the package when offered by the carrier for delivery and,
2. monitor external surfaces of the conveyance and package for radioactive contamination and radiation levels.

All users shall include provisions for reporting safety concerns associated with the packaging or its use. The user shall notify NRC in accordance with 10 CFR 20.2202. Incidents requiring notification include:

1. removable radioactive surface contamination in excess of the limits provided by 10 CFR 71.87, and
2. external radiation levels in excess of the limits provided by 10 CFR 71.47.

The receiver shall compare the cargo with the list provided by the shipper. If a discrepancy appears between the cargo and the list, the receiver shall investigate and report to the NRC as required.

The package shall be removed from the conveyance prior to unloading the content. Unloading procedures shall, at a minimum, ensure that:

1. the package nonfixed surface contamination is below the minimum on-site or off-site requirements,
2. all appropriate package labels are affixed to the package exterior surface,
3. all lifting and handling equipment is certified for use,
4. all transfer equipment is certified for use,
5. the package is visually examined to ascertain surface damage that may have occurred during shipping or handling, and
6. the TIDs are examined to ensure that the package has not been tampered with during shipment.